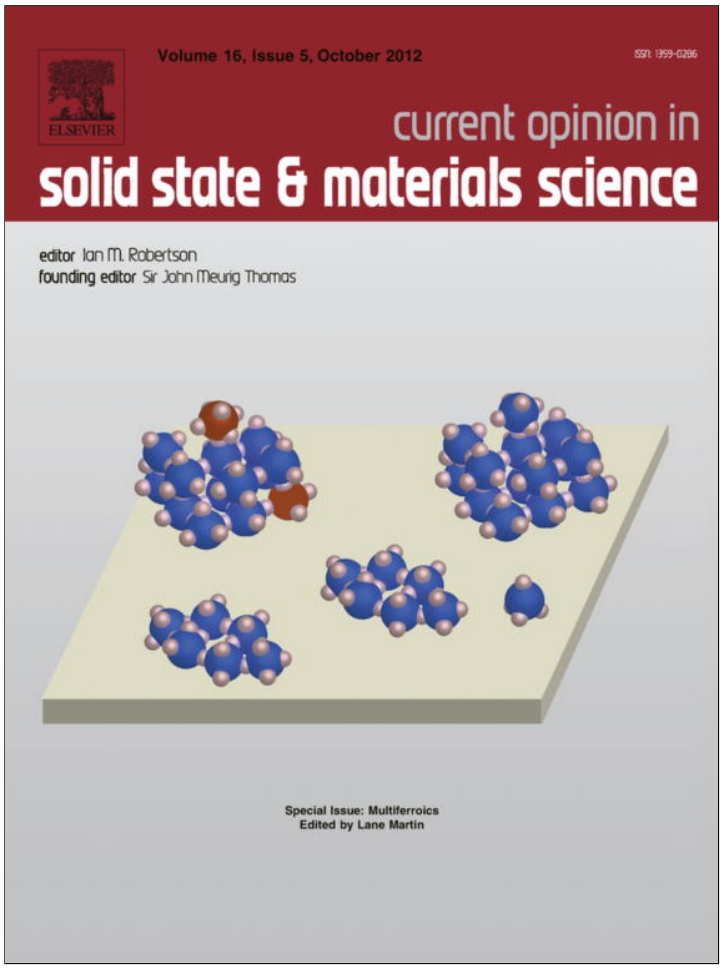

Current Opinion in Solid State and Materials Science 16 (2012) 199–215

Contents lists available at SciVerse ScienceDirect

Current Opinion in Solid State and Materials Science

journal homepage: www.elsevier.com/locate/cossms

Advanced synthesis techniques and routes to new single-phase multiferroics

Lane W. Martin [a,*], Darrell G. Schlom [b]

[a] Department of Materials Science and Engineering and Materials Research Laboratory, University of Illinois, Urbana-Champaign, Urbana, IL 61801, United States
[b] Department of Materials Science and Engineering, Cornell University, Ithaca, NY 14853, United States

ARTICLE INFO

Article history:
Available online 27 March 2012

Keywords:
Multiferroic
Pulsed-laser deposition
Molecular beam epitaxy
$BiFeO_3$
$EuTiO_3$
Magnetoelectric
Thin films
Strain-engineering

ABSTRACT

We review recent developments and advances in the synthesis of thin-film multiferroic and magnetoelectric heterostructures. Driven by the promise of new materials with built-in useful phenomena (i.e., electric field control of ferromagnetism), extensive research has been centered on the search for and characterization of new single-phase multiferroic materials. In this review we provide a brief overview of recent developments in the synthesis of thin film versions of these materials. Advances in modern film growth processes have provided access to high-quality materials for in-depth study. We highlight the use of epitaxial thin-film strain to stabilize metastable phases, drive multiferroic properties, and produce new structures and properties in materials including case studies of $EuTiO_3$ and $BiFeO_3$.

1. Introduction

1.1. Overview

Complex oxides represent a broad class of materials that have a wide range of crystal structures and properties. Among them, the study of magnetic, ferroelectric, and, more recently, multiferroic properties has stimulated considerable interest. This work has been driven, in part, by the development of new thin-film growth techniques and the access to high-quality materials that has resulted. In this review, we focus on the synthesis of thin films of these materials and routes to control these properties with special attention to the use of epitaxial thin-film strain. Such epitaxial strain can give rise to complex and diverse physical phenomena that result from the coupling of lattice, orbital, spin, and charge degrees of freedom.

Creating novel materials is thus a critical component that enables the exploration of such fascinating phenomena. The power of advanced materials synthesis has been repeatedly demonstrated in materials science. For example, in semiconductor epitaxy, advanced thin-film synthesis has led to not only a large range of technologies, but has also led to several Nobel prizes. Researchers in oxide and multiferroic science have taken a page out of the semiconductor lexicon and consequently, materials synthesis plays a critical role in enabling the study of such novel materials. In this article, recent advances in the synthesis of epitaxially strained multiferroic and magnetoelectric oxide materials (in particular systems such as $EuTiO_3$ and $BiFeO_3$) are reviewed. We highlight the importance of advanced synthesis techniques and the interplay between synthesis, theory, and experimental probes [2].

1.2. Multiferroic materials systems

Metal oxide materials have been the focus of much research based on the broad range of structures, properties, and exciting phenomena that are manifested in these materials [3,4]. The perovskite structure, which has the chemical formula ABO_3 (e.g., $CaTiO_3$, $SrRuO_3$, $BiFeO_3$) (Fig. 1), is made up of corner-sharing octahedra with the *A*-cation coordinated with twelve oxygen ions and the *B*-cation with six. The structure can easily accommodate a wide range of valence states on both the *A*- and *B*-sites (i.e., $A^{+1}B^{+5}O_3$, $A^{+2}B^{+4}O_3$, $A^{+3}B^{+3}O_3$) and can exhibit complex defect chemistry (including accommodation of a few percent of cation non-stoichiometry, large concentrations of oxygen vacancies, and exotic charge accommodation modes ranging from disproportionation to cation ordering) [5]. Selection of the appropriate *A*- and *B*-site cations can dramatically impact structural, electronic, magnetic, polar, and other properties. In the end, the electronic structure and coordination chemistry of the cationic species control the wide range of physical phenomena manifested in these materials.

1.2.1. Multiferroics – definition

Over the past several years, the exploration of these individual functional responses has evolved into the exploration of coupled order, namely the existence of multiple order parameters, as exemplified by multiferroics. By definition, a single-phase multiferroic

* Corresponding author. Tel.: +1 217 244 9162; fax: +1 217 333 2736.
E-mail address: lwmartin@illinois.edu (L.W. Martin).

1359-0286/$ - see front matter © 2012 Elsevier Ltd. All rights reserved.
http://dx.doi.org/10.1016/j.cossms.2012.03.001

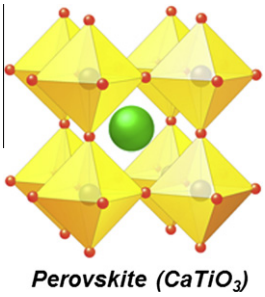

Fig. 1. Representation of the perovskite (ABO_3) crystal structure. The prototype material $CaTiO_3$ is shown with Ca-ions shown in green, Ti-ions in light blue, and O-ions in red.

[6] is a material that simultaneously possesses two or more of the so-called "ferroic" order parameters: ferroelectricity, ferromagnetism, and/or ferroelasticity (note that the current trend is to extend the definition to include materials possessing the corresponding antiferroics as well, e.g., antiferromagnetic ferroelectrics such as $BiFeO_3$, as there are so few ferromagnetic ferroelectrics). Magnetoelectric coupling typically refers to the linear magnetoelectric effect manifested as an induction of magnetization by an electric field or polarization by a magnetic field [7]. Only a small subgroup of all magnetically and electrically polarizable materials are either ferromagnetic or ferroelectric and fewer still simultaneously exhibit both order parameters (Fig. 2) [8]. The ultimate goal for device functionality is a single-phase multiferroic with strong coupling between ferroelectric and ferromagnetic order parameters enabling electric field control of magnetism.

1.2.2. Scarcity of and pathways to multiferroism

Multiferroics are a rather rare set of materials. The scarcity of multiferroics can be understood by investigating a number of factors including symmetry, electronic properties, and chemistry. First, only 13 of the Shubnikov–Heesch point groups (out of 122) are compatible with multiferroic behavior. Specifically, these are 1, 2, 2′, *m*, *m*′, 3, 3*m*′, 4, 4*m*′*m*′, *m*′*m*2, *m*′*m*′2, 6, and 6*m*′*m*′ [6]. Additionally, ferroelectrics by definition are insulators and in 3*d* transition metal oxides, typically possess *B*-cations that have a formal d^0 electronic state, while itinerant ferromagnets possess unpaired electrons (even in double exchange ferromagnets such as the manganites, magnetism is mediated by incompletely filled 3*d* shells). Thus there exists a seeming contradiction between the conventional mechanism of off-centering in a ferroelectric and the formation of magnetic order, which explains the scarcity of ferromagnetic–ferroelectric multiferroics [9]. There are a number of pathways, however, that have been observed to give rise to multiferroic properties (Table 1 briefly summarizes some examples). In general, multiferroics can be divided into one of two groups [10]. Type I multiferroics are materials in which ferroelectricity and magnetism have different sources and appear largely independent of one another as is the case in $BiFeO_3$ [11], $YMnO_3$ [12], and $LuFe_2O_4$ [13]. On the other hand, Type II multiferroics are materials in which magnetism causes ferroelectricity – implying a strong coupling between the two order parameters. The prototypical examples of this sort of behavior are $TbMnO_3$ [14] and $TbMn_2O_5$ [15].

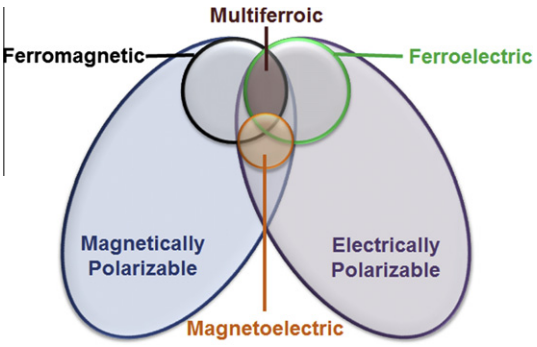

Fig. 2. (a) Relationship between multiferroic and magnetoelectric materials. Illustrates the requirements to achieve both in a material (adapted from Ref. [8]).

1.2.3. Alternative pathways to magnetoelectricity

Because of the rare nature of multiferroism, researchers have investigated alternative pathways by which to achieve the sought after effects made possible by these materials including considerable work in the area of composite magnetoelectric systems. A complete treatment of this rich field is beyond the scope of this manuscript, but here we highlight a few of major discoveries. For a thorough treatment of this field the reader is directed to Refs. [16–18]. Composite magnetoelectrics operate by coupling the magnetic and electric properties between two materials, generally a ferroelectric material and a ferrimagnetic material, via strain. An applied electric field creates a mechanical strain in the ferroelectric via the converse piezoelectric effect, which produces a corresponding strain in the ferrimagnetic material and a subsequent change in magnetization or the magnetic anisotropy via the piezomagnetic effect. Work started in the field several decades ago using bulk composites [19–21]. Experimental magnetoelectric voltage coefficients were far below those calculated theoretically [22]. This suggested the possibility for strong magnetoelectric coupling in a multilayer (2–2) configuration [23] – an ideal structure to be examined by the burgeoning field of complex oxide thin-film growth [24]. In this spirit, researchers experimentally tested a number of materials in a laminate thick-film geometry, including ferroelectrics such as $Pb(Zr_x,Ti_{1-x})O_3$ [25–30], $Pb(Mg_{0.33}Nb_{0.67})O_3$–$PbTiO_3$ (PMN-PT) [31], and ferromagnets such as $TbDyFe_2$ (Terfenol-D) [25], $NiFe_2O_4$ [26,28], $CoFe_2O_4$ [30], $Ni_{0.8}Zn_{0.2}Fe_2O_4$ [27], $La_{0.7}Sr_{0.3}MnO_3$ [29], $La_{0.7}Ca_{0.3}MnO_3$ [29], and others. These experiments showed great promise and magnetoelectric voltage coefficients up to $\Delta E/\Delta H = 4680$ mV/cm Oe have been observed. In general, however, it is thought that the in-plane magnetoelectric interface of such heterostructures limits the magnitude of the coupling coefficient due to the clamping effect of the substrate on the ferroelectric phase [32]. Since the amount of strain that can be imparted by the ferroelectric phase is limited via this in-plane interfacial geometry, the magnetoelectric voltage coefficient can be reduced by up to a factor of five.

This has, in turn, lead to the study of *vertical nanostructures* to enhance coupling. A seminal paper by Zheng et al. [33] showed that magnetoelectric materials could also be fabricated in a nanostructured columnar fashion by selecting materials that spontaneously separate due to immiscibility, such as spinel and perovskite phases [22]. This results in nanostructured phases made of pillars of one material embedded in a matrix of another. In this initial paper, researchers reported structures consisting of $CoFe_2O_4$ pillars embedded in a $BaTiO_3$ matrix. The large difference in lattice parameter between these phases leads to the formation of pillars with dimensions on the order of tens of nanometers, which ensures a high interface-to-volume ratio, an important parameter when attempting to couple the two materials via strain. These nanostructures, in which the interface is perpendicular to the substrate, remove the effect of substrate clamping and allow for better strain-induced coupling between the two phases. Nanostructured composites with combinations of a number of perovskite ($BaTiO_3$ [34], $PbTiO_3$ [35], $Pb(Zr_x,Ti_{1-x})O_3$ [36,37], and $BiFeO_3$ [38,39]) and spinel ($CoFe_2O_4$ [36,37], $NiFe_2O_4$ [35,38], and γ-Fe_2O_3 [39]) or corundum (α-Fe_2O_3 [39]) structures have been investigated.

Table 1
Summary of pathways to multiferroic order in materials including various Type I and II routes and prototypical materials.

	Pathway to	Mechanism for multiferroism	Examples
Type I	A-site driven	Stereochemical activity of *A*-site lone pair gives rise to ferroelectricity and magnetism arises from *B*-site cation	$BiFeO_3$, $BiMnO_3$
	Geometrically driven	Long-range dipole–dipole Interactions and oxygen rotations drive the system towards a stable ferroelectric state	$YMnO_3$, $BaNiF_4$
	Charge ordering	Non-centrosymmetric charge ordering arrangements result in ferroelectricity in magnetic materials	$LuFe_2O_4$
Type II	Magnetic ordering	Ferroelectricity is induced by the formation of a symmetry-lowering magnetic ground state that lacks inversion symmetry	$TbMnO_3$, $DyMnO_3$, $TbMn_2O_4$

2. Advances in the growth of multiferroic thin films

The re-emergence of interest in multiferroics has been driven, in part, by the development of thin-film growth techniques that allow for the production of non-equilibrium phases of materials and strain engineering of existing materials [40,41]. Thin films offer a pathway to the discovery and stabilization of a number of new multiferroics in conjunction with the availability of high quality materials that can be produced with larger lateral sizes than single crystal samples. In turn, this has offered researchers unprecedented access to new phases and insight about these materials. In this section we discuss recent advances in the growth of multiferroic thin films.

2.1. The power of epitaxial thin-film strain

For at least 400 years mankind has studied the effect of pressure (hydrostatic strain) on the properties of materials [42]. In the 1950s it was shown that biaxial strain, where a film is clamped to a substrate, but free in the out-of-plane direction, can alter the transition temperatures of superconductors [43] and ferroelectrics [44].

What has changed in recent years is the magnitude of the biaxial strain that can be imparted. Bulk multiferroic oxides are brittle and will crack under moderate tensile strains, typically 0.1%. Under compressive strains they begin to plastically deform (or break) under comparable strains [45]. One way around this limitation is the approach of bulk crystal chemists: to apply "chemical pressure" through isovalent cation substitution. A disadvantage of such a bulk approach, however, is the introduction of disorder and potentially unwanted local distortions. Epitaxial strain, the trick of the thin-film alchemist, provides a potentially disorder-free route to large biaxial strain and has been used to greatly enhance the mobility of transistors [46,47] and significantly increase superconducting [48,49], ferromagnetic [50–52], and ferroelectric [53–55] transition temperatures. Strains of about ±3% are common in epitaxial multiferroics today [56–59], with the record to date being a whopping 6% compressive strain achieved in thin $BiFeO_3$ films grown on (1 1 0) $YAlO_3$ [60–62]. These strains are an order of magnitude higher than where these materials would crack or plastically deform in bulk [63–65].

Fully coherent, epitaxial films also have the advantage that high densities of threading dislocations (e.g., the $\sim 10^{11}$ dislocations cm^{-2} observed, for example, in partially relaxed $(Ba_xSr_{1-x})TiO_3$ films) [66,67] are avoided. Strain fields around dislocations locally alter the properties of a film, making its ferroelectric properties inhomogeneous and often degraded [68–70]. Of course to achieve highly strained multiferroic films and keep them free of such threading dislocations one needs to keep them thin, typically not more than a factor of five beyond the Matthews–Blakeslee equilibrium limit [65]. Thickness-dependent studies involving the growth of a multiferroic on a single type of substrate to study the effect of strain in partially relaxed films are not as clean as using commensurate films grown on different substrates. In the former the strains are inhomogeneous and the high concentration of threading dislocations can obfuscate intrinsic strain effects.

The combination of advances in predictive theory with the ability to customize the structure and strain of oxide heterostructures at the atomic-layer level has enabled a new era: multiferroics by design. One success story of this approach is $EuTiO_3$, a ferroelectric ferromagnet predicted [71] to be the strongest known multiferroic with a spontaneous polarization and spontaneous magnetization each 100× superior to the reigning multiferroic it displaced, $Ni_3B_7O_{13}I$ [72,73]. First principles theory predicted [71] that this normally boring paraelectric and antiferromagnetic insulator (in its unstrained bulk state) could be transformed into a colossal multiferroic with appropriate strain and this was indeed found to be the case [59]. There are more recent predictions (remaining to be verified) of even stronger and higher temperature ferroelectric ferromagnets in strained $SrMnO_3$ [74] and EuO [75] as well as the prediction that an electric field of order 10^5 V/cm can be used to turn on ferromagnetism in $EuTiO_3$ when it is poised on the verge of such a phase transition via strain [71]. Never has it been possible to turn on magnetism in a material by applying an *electric* field to it. Such an important milestone would be a key advance to the field of multiferroics, both scientifically and technologically. Electronics has flourished because of the ability to route voltages with ease and on extremely small scales. If magnetism could be similarly controlled and routed, it would impact memory devices, spin valves and many other spintronics devices, and make numerous hybrid devices possible. Testing these predictions requires substrates that can impart the needed biaxial strain.

Fortunately for the case of perovskite multiferroics many isostructural substrates exist with a broad range of lattice parameters to impart a desired strain state into the overlying film. The substrate situation for non-perovskite multiferroics is not nearly as favorable. The status of which perovskite single crystals are available commercially with substrate sizes of at least 10 mm × 10 mm together with the pseudocubic lattice parameters of multiferroic and related perovskite phases of interest is shown in Fig. 3. These single crystal perovskite and perovskite-related substrates are $LuAlO_3$ [76,77], $YAlO_3$ [78], $LaSrAlO_4$ [79], $NdAlO_3$ [80], $LaAlO_3$ [81,82], $LaSrGaO_4$ [83], $(NdAlO_3)_{0.39}$–$(SrAl_{1/2}Ta_{1/2}O_3)_{0.61}$ (NSAT) [84], $NdGaO_3$ [85,86], $(LaAlO_3)_{0.29}$–$(SrAl_{1/2}Ta_{1/2}O_3)_{0.71}$ (LSAT) [84,87], $LaGaO_3$ [88], $SrTiO_3$ [89–92], $Sr_2(Al,Ga)TaO_6$ (SAGT), $DyScO_3$ [93], $TbScO_3$ [94], $GdScO_3$ [93], $EuScO_3$, $SmScO_3$ [93], $KTaO_3$ [95], $NdScO_3$ [93], and $PrScO_3$ [96]; many of these substrates can be produced with structural perfection rivaling that of conventional semiconductors. The perfection of the substrate, the best of which are grown by the Czochralski method (which is not applicable to most multiferroics because they do not melt congruently), can be passed on to the film via epitaxy. This has led to the growth of epitaxial films of $BiFeO_3$ [97], $BiMnO_3$ [98], and strained $EuTiO_3$ [59] with rocking curve full width at half maximum (FWHM) ⩽ 11 arcsec (0.003°)—values within instrumental error identical to those of the commercial substrates upon which they are grown and significantly narrower (indicative of higher structural perfection) than the most perfect single crystals of these same materials.

For the growth of high quality multiferroic films with a desired strain state, not only are appropriate substrates needed, but also methods to prepare smooth and highly perfect surfaces with

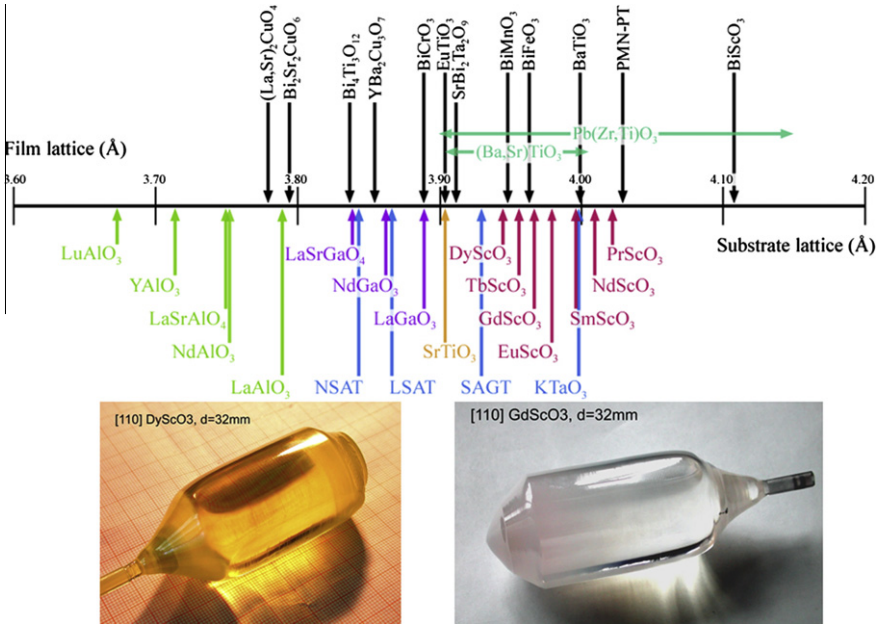

Fig. 3. A number line showing the pseudotetragonal or pseudocubic *a*-axis lattice constants in angstroms of some perovskites and perovskite-related phases of interest including multiferroics (above the number line) and of some of the perovskite and perovskite-related substrates that are available commercially (below the number line). The photos of exemplary single crystals used as substrates are from Ref. [96].

ideally a specific chemical termination on which epitaxial growth can be initiated. For example, chemical-mechanically polished (001) $SrTiO_3$ substrates display a mixture of SrO and TiO_2 terminated surfaces. Kawasaki et al. [99] showed that an NH_4F-buffered HF solution with controlled pH enables etching of the more basic SrO layer and leaves a completely TiO_2-terminated surface on the substrate [99]. This method of preparing a TiO_2-terminated (001) $SrTiO_3$ surface has been further perfected by Koster et al. [100]. SrO-terminated (001) $SrTiO_3$ substrates can also be prepared [101]. A means to prepare low defect surfaces with controlled termination has also been developed for (110) $SrTiO_3$ [102], (111) $SrTiO_3$ [102,103], $(001)_p$ $LaAlO_3$ [104,105], $(111)_p$ $LaAlO_3$ [104], (110) $NdGaO_3$ [105], $(001)_p$ LSAT, [105,106] (110) $DyScO_3$ [107], (110) $TbScO_3$ [107], (110) $GdScO_3$ [107], (110) $EuScO_3$ [107], (110) $SmScO_3$ [107], $KTaO_3$ [108], (110) $NdScO_3$ [107], and (110) $PrScO_3$ [107] substrates. Here the *p* subscript refers to pseudocubic indices.

2.2. Thin-film growth techniques

2.2.1. Molecular beam epitaxy

MBE is a vacuum deposition method in which well-defined thermal beams of atoms or molecules react at a crystalline surface to produce an epitaxial film. It was originally developed for the growth of GaAs and (Al,Ga)As [109], but due to its unparalleled ability to control layering at the monolayer level and compatibility with surface-science techniques to monitor the growth process as it occurs, its use has expanded to other semiconductors as well as metals and insulators [110,111]. Epitaxial growth, a clean ultra-high vacuum (UHV) deposition environment, *in situ* characterization during growth, and the notable absence of highly-energetic species are characteristics that distinguish MBE from other methods used to prepare thin films of complex oxides and multiferroics. These capabilities are key to the precise customization of complex oxide heterostructures at the atomic layer level. MBE is traditionally performed in UHV chambers to avoid impurities. In addition to molecular beams emanating from heated crucibles containing individual elements, molecular beams of gases may also be introduced, for example to form oxides or nitrides. This variant of MBE is known as "reactive MBE" [112] in analogy to its similarity to "reactive evaporation," which takes place at higher pressures where well-defined molecular beams are absent. Reactive evaporation has also been extensively used to grow complex oxide films [113], but here we limit our discussion to reactive MBE. Another popular variant of MBE is the use of volatile metalorganic source materials; this is called metal-organic MBE (MOMBE) and is being applied to an increasing variety of complex oxides [114–116].

While there are many ways to grow epitaxial oxide films, reactive MBE has the advantage of being able to prepare films of the highest quality and with unparalleled layering control at the atomic-layer level. This includes phases and perfection that are not achievable by other techniques. A few examples are (1) the epitaxial growth of $SrTiO_3$ on (100) Si [55,117–126], which has not been achieved by any other technique to date despite the 20 year history of this system, (2) the growth of ZnO with the highest mobility to date [127,128] (over 125 times higher than achieved by any other technique) [129] as expected considering that MBE has provided the highest mobility in III–V heterostructures for decades [130–132], and (3) the growth of thin films with the narrowest X-ray diffraction rocking curves (highest structural quality) ever reported for any oxide film grown by any technique [133–136].

MBE is renowned for its unparalleled structural control in the growth of compound semiconductor microstructures where MBE has provided nanoscale thickness control and exceptional device characteristics for decades. Examples of the thickness control achieved in semiconductors include interspersing layers as thin as one monolayer (0.28 nm) of AlAs at controlled locations into a GaAs film [137] and alternating monolayers of GaAs and AlAs to make a one-dimensional superlattice [138]. This nanoscale control has enabled tremendous flexibility in the design, optimization, and manufacturing of new devices, especially those making use of quantum effects [139]. Such control has also been demonstrated by MBE for the synthesis of complex oxide superlattices with atomic-scale thickness control and abrupt interfaces [41,140–148] and the construction of new complex oxide phases with atomic layer precision [41,142,149–151]. These advances in thin film deposition technology have made it possible to customize oxide heterostructures with sub-nanometer precision.

Additional advantages of MBE are (1) completely independent control of the sequence in which the elemental constituents are supplied to the substrate, (2) the availability of high purity elemental source materials, (3) no boundary layers or complicated precursor reaction chemistries, and (4) it is a very low energy, gentle deposition process in which neutral depositing species arrive at the substrate with energies well under 1 eV from the thermally generated molecular beams. The literature of film growth is riddled with examples in which bombardment by high energy species results in extrinsic film properties [152–157]. MBE is a thin film preparation technique for complex oxides that allows their intrinsic properties to be explored.

The controlled growth of multicomponent oxides is crucially dependent on accurate composition control. Inadequate composition control has been a major problem for previous oxide molecular beam epitaxy (MBE) work [142]. Although improvements in flux measurement methods continue to occur, an advantage of many multiferroics is that they contain volatile species (e.g., bismuth) and can be growth in an adsorption-controlled regime where composition control is automatic. This thermodynamically established process is responsible for the precise composition achieved in films of GaAs and other compound semiconductors by MBE and MOCVD, despite their being immersed in a huge overpressure of arsenic-containing species during growth. Thermodynamic calculations have aided the identification of the growth window for the adsorption-controlled growth of $BiFeO_3$ [97,158], $BiMnO_3$ [98], and their solid solution [159]. In the case of multiferroic oxides containing a volatile constituent, oxygen background pressure and substrate temperature are the parameters that define the growth window where stoichiometric film deposition occurs.

2.2.2. Pulsed-laser deposition

No other single advance in the synthesis of oxide materials has had as deep an impact as the wide-spread implementation of laser-ablation-based growth techniques. The reader is directed to a number of excellent books and thorough reviews on the history and evolution of this process [160–162]. Pulsed-laser deposition (PLD) moved complex oxide synthesis from work focused on bulk single crystals and powder samples, to high-quality thin films. Additionally, PLD is a far from equilibrium process and, with careful control, can preserve complex stoichiometry from target to film. It is also a flexible, high-throughput process, ideal for the research laboratory where rapid prototyping of materials and investigating a wide array of phase space is necessary.

Briefly, PLD is a rather simple thin film growth process that can be carried out in reactive environments, like that for oxides where a partial pressure of oxygen, ozone, or atomic oxygen is carefully controlled. One of the aspects of PLD that makes it such a versatile growth process is that the deposition is achieved by vaporization of materials by an external energy source – the laser.

There have been a number of recent advances in PLD and great strides have been made in utilizing the unique features of PLD to create new multiferroics. One example is the automation of systems to enable alloy formation from multiple targets which has been used to make multiferroics such as $Bi(Fe_{1-x}Cr_x)O_3$ [163]. Using new hardware, PLD can also be used to synthesize precisely controlled interfaces in materials that rival the capabilities of MBE. This has been particular aided by the development of differentially pumped reflection high-energy electron diffraction (RHEED) systems that have allowed researchers to monitor growth processes in high partial pressures of gases (>200–300 mTorr in some cases) [164,165], has enabled sequential growth of binary oxide materials [166], and has allowed highly controlled layer-by-layer growth [167–169]. Such advances have enabled increased study of interfacial properties and interactions in complex oxides and multiferroics. Additionally, advances have been made in obtaining information from RHEED studies including a technique known as RHEED–TRAXS (total-reflection-angle X-ray spectroscopy) [170]. In this process, incident RHEED electrons collide with the atoms in the sample, knocking secondary electrons out of their shells. Electrons in the outer shells drop into the empty inner shells, emitting X-rays whose energies are characteristic of the species of atoms in the growing film. The RHEED beam that strikes the sample thus creates a spectrum of X-rays and collecting and analyzing the emitted X-rays provides details about the species of atoms in the growing film and surface stoichiometry. Other *in situ* characterization of oxide materials can be done via time-of-flight ion scattering and recoil spectroscopy (ToF-ISARS) [171–174]. ToF-ISARS is a non-destructive, *in situ*, real-time probe of thin film composition and structure which does not interfere with the growth process. An review of the technique is given in Ref. [171], but briefly it utilizes a low-energy (5–15 keV) pulsed ion beam surface analysis process that can give information on surface composition, the atomic structure of the first few monolayers, trace element detection, lattice defect density, mean vibrational amplitude, and information on thickness and lateral distribution of the growth region. Recent studies have relied on ToF-ISARS to characterize the nature of interfaces with sub-unit-cell precision [175].

There has also been a recent push to integrate other characterization techniques with PLD (and MBE) growth systems. This includes combining X-ray photoelectron spectroscopy (XPS), scanning probe measurements systems (including atomic force microscopy (see work by the Twente group) [176], piezoresponse force microscopy, magnetic force microscopy, scanning tunneling microscopy, etc.), and synchrotron-based techniques with growth chambers. At the Photon Factory in Tsukuba, Japan researchers have created a high-resolution synchrotron-radiation angle-resolved photoemission spectrometer (ARPES) combined with a combinatorial RHEED-assisted PLD system [177], time-resolved X-ray diffraction studies of the PLD process have also been completed at the Advanced Photon Source [178,179], and other similar systems have since been constructed at the European Synchrotron Radiation Facility in Grenoble, France [180] and at the Cornell High Energy Synchrotron Source (CHESS) [181].

2.2.3. Others techniques: sputtering, MOCVD, and ALD

Recently a number of other growth techniques have been used to synthesize multiferroic thin films. Sputtering is a widely used deposition technique for large-scale production. With the advent of multi-source deposition, significant advances in sputtering of complex chemical composition materials have been obtained [182]. Sputtering has been used to grow multiferroics such as $YMnO_3$ [183], $BiFeO_3$ [184], and others. Metal–organic chemical vapor deposition (MOCVD) is also of great importance for large-scale production of oxide thin films [185]. With the advent of new metal–organic precursors for elements with high atomic number (which typically have limited vapor pressure at room temperature) access to multiferroic materials has been demonstrated. This was especially important in the development of MOCVD grown $BiFeO_3$ [186]. The reader is directed a review of recent work on the deposition of multiferroics from metalorganics [187]. More recently, the use of atomic layer deposition (ALD) has become important for the controlled synthesis of oxide films. ALD relies on two self-limiting reactions between gas-phase precursor molecules and a solid surface and differs from standard CVD or MOCVD, where there is mixing and thus reaction of precursor gases prior to the substrate. ALD lends itself to more precisely grown films due to the ability to control the order in which gases arrive. Early work has demonstrated the promise of this technique for the growth of complex oxides $PbZr_{1-x}Ti_xO_3$ [188] and select manganites [189]. As of submission of this manuscript, few reports of

the ALD growth of multiferroics are available [190,191] including extensive investigation of some manganites [192].

3. Changing the materials landscape – heteroepitaxy of single-phase multiferroics

3.1. Thin-film multiferroics

A number of multiferroic thin films have been synthesized and studied, but a detailed treatment of this extensive work is beyond the scope of this manuscript. Here we recap some of the work on thin-film multiferroics in the last few years. The earliest multiferroic thin films to be studied were the rare-earth manganites (*RE*-MnO_3) which are an intriguing system because depending on the size of the *RE* ion the structure takes on either orthorhombic (*RE* = La–Dy; only *RE* = Dy, Tb, and Gd are multiferroic and have very low (~20–30 K) ferroelectric ordering temperatures [14,193]) or hexagonal (*RE* = Ho–Lu, as well as Y; all exhibit multiferroic behavior with relatively high ferroelectric ordering temperatures and relatively low magnetic ordering temperatures [194]) structures [195]. Recently the *RE*Mn_2O_5 (*RE* = rare earth, Y, and Bi) family of materials has also received attention as thin films for the first time [196]. Researchers have investigated ferroelectric stability in ultra-thin layers of these materials [197], have used such multiferroic manganites to demonstrate electric field control of exchange coupled ferromagnets [198], and have investigated the effects of non-stoichiometry and solubility limits [199].

$BiMnO_3$, which has also received considerable attention, is not a stable phase at 1 atm pressure and its synthesis in bulk form requires high pressure and high temperatures (on the order of 6 GPa at around 1100 K) [200–202]. An alternative approach to synthesize $BiMnO_3$ is to use epitaxial stabilization and lattice misfit strain and interfacial energies to favor the desired metastable phase over the equilibrium phase. Utilizing epitaxial stabilization $BiMnO_3$ thin films were first grown on $SrTiO_3$ (001) single crystal substrates using PLD [203]. Bulk $BiMnO_3$ has been reported to belong to polar space group *C2* below ~450 K and undergoes an unusual orbital ordering leading to ferromagnetism at ~105 K [204] while films exhibit a substrate-dependent ferromagnetic transition temperature [205]. $BiMnO_3$ has been used as the foundation for a four-state memory concept [206] and has been shown to exhibit large magnetodielectric effects [207]. Recent first-principles calculations [208] and structural refinements [209], however, find that stoichiometric $BiMnO_3$ belongs to the centrosymmetric *C*2/*c* space group. If correct, this would mean that $BiMnO_3$ is neither ferroelectric nor multiferroic.

There are a number of other candidate multiferroic materials that have been studied as thin films. $BiCrO_3$ has been predicted to be multiferroic [210] and thin films of $BiCrO_3$ have been grown on a variety of substrates and have been shown to be antiferromagnetic (with weak ferromagnetism) with an ordering temperature of ~120–140 K. Early reports suggested that these films showed piezoelectric response and a tunable dielectric constant at room temperature [211] while others suggested that the films were antiferroelectic as predicted in theory [212]. Bulk work on $BiCoO_3$ [213] and theoretical predictions of giant electronic polarization of more than 150 μC/cm^2 [214] have driven researchers to attempt creating films of this phase. To date, however, only solid solutions of $BiFeO_3$–$BiCoO_3$ have been grown [215,216]. Another phase of interest is $PbVO_3$ [217]. $PbVO_3$ films were grown on a range of substrates and were found possess a highly tetragonal perovskite phase with a *c*/*a* lattice parameter ratio of 1.32 (Fig. 4). Further analysis of this material using second harmonic generation and X-ray dichroism measurements revealed that $PbVO_3$ is both a polar, piezoelectric and likely antiferromagnetic below ~130 K [218]. There has also been attention given to double-perovskite structures such as Bi_2NiMnO_6 which have been shown to be both ferromagnetic ($T_C \sim 100$ K) and ferroelectric with spontaneous polarization of ~5 μC/cm^2 [219].

3.2. Recent advances – strain-induced effects in multiferroics

3.2.1. Strain-induced multiferroics

Recently, Fennie and Rabe proposed a new route to ferroelectric ferromagnets [71]—transforming magnetically ordered insulators that are neither ferroelectric nor ferromagnetic, of which there are many, into ferroelectric ferromagnets using epitaxial strain. The work investigated $EuTiO_3$ which was predicted to simultaneously exhibit strong ferromagnetism ($M_s \sim 7\ \mu_B$/Eu) and strong ferroelectricity ($P_s \sim 10$ μC/cm^2) under sufficiently large biaxial strain [71]. These values are orders of magnitude higher than any known ferroelectric ferromagnet and rival the best materials that are solely ferroelectric or ferromagnetic. To test these predictions, commensurate $EuTiO_3$ films were grown on three substrates: (001) LSAT, (001) $SrTiO_3$, and (110) $DyScO_3$ to impart −0.9%, 0%, and +1.1% biaxial strain, respectively. Experimental measurements (Fig. 5) confirmed that the $EuTiO_3$/$DyScO_3$ was simultaneously ferromagnetic and ferroelectric, while on the other substrates it was not. This work demonstrated that a single experimental parameter, strain, simultaneously controls multiple order parameters and is a viable alternative tuning parameter to composition for creating multiferroics.

The physics behind this discovery makes use of spin-phonon coupling as an additional parameter to influence the soft mode of an insulator on the verge of a ferroelectric transition. Appropriate materials are those (1) with a ground state in the absence of strain that is antiferromagnetic and paraelectric, (2) on the brink of a ferroelectric transition (incipient ferroelectrics), and (3) with a large spin-phonon coupling [71]. $EuTiO_3$ meets these three criteria and has much in common with $SrTiO_3$ except that $EuTiO_3$ magnetically

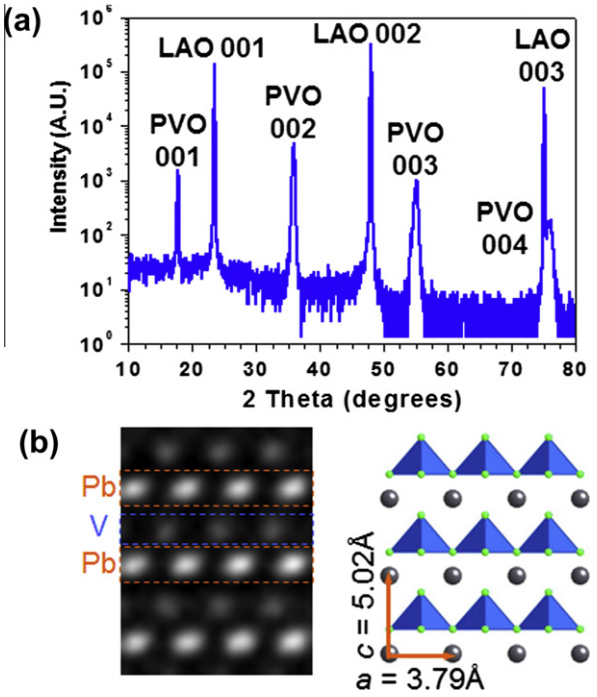

Fig. 4. (a) X-ray diffraction of a fully epitaxial $PbVO_3$/$LaAlO_3$ (001) thin film. (b) High resolution, cross-sectional transmission electron microscopy image of the $PbVO_3$ structure along with a schematic illustration of the large *c*/*a* lattice parameter distortion in this super tetragonal phase. (Adapted from Ref. [217]).

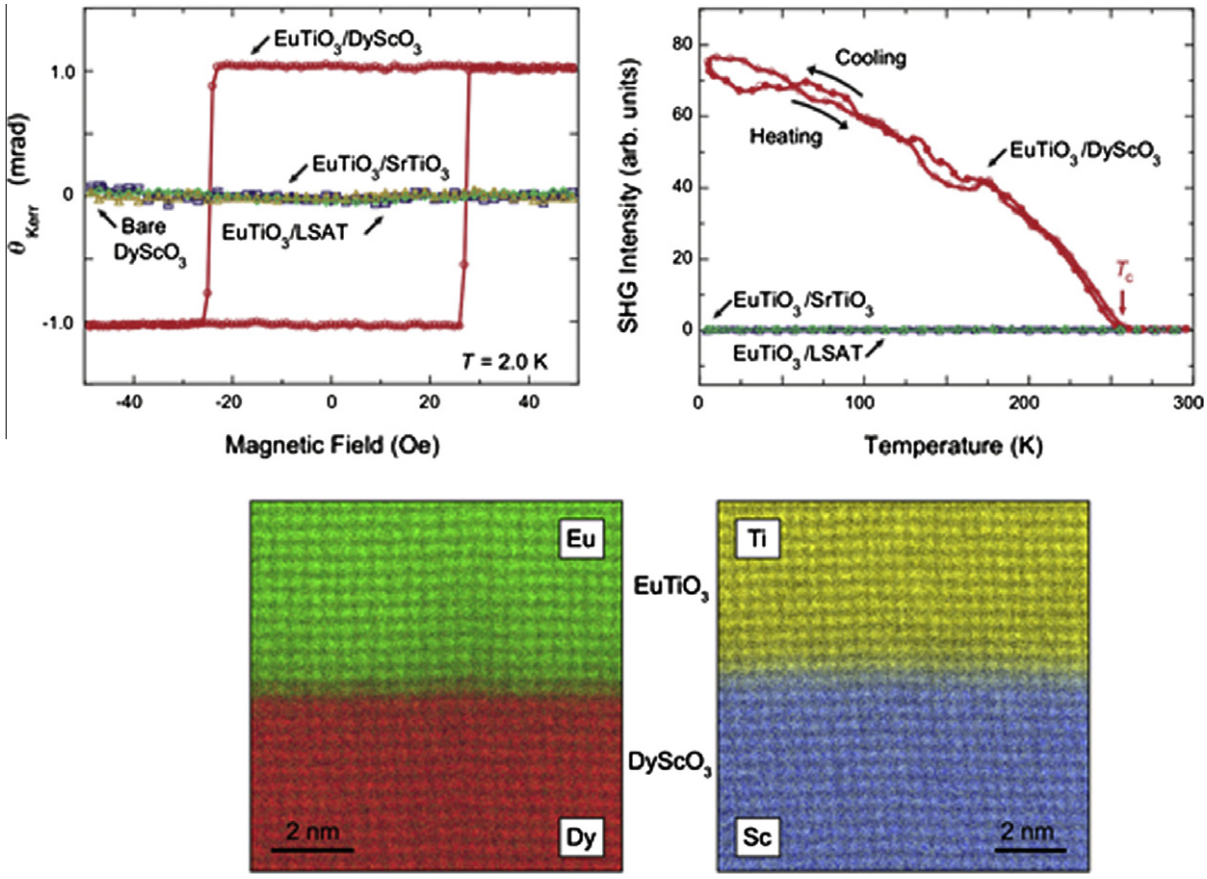

Fig. 5. Observation of ferromagnetism by MOKE and ferroelectricity by SHG in strained $EuTiO_3$ grown on (110) $DyScO_3$, confirming predictions that under sufficient biaxial strain $EuTiO_3$ becomes multiferroic. Control samples with zero ($EuTiO_3/SrTiO_3$) or opposite ($EuTiO_3$/LSAT) strain are consistent with the theoretically predicted strain phase diagram for $EuTiO_3$. Elemental maps of Eu and Dy as observed by STEM-EELS on the same $EuTiO_3/DyScO_3$ film, confirming an abrupt $EuTiO_3/DyScO_3$ interface with the correct oxidation states (from Ref. [59]).

orders at 5 K due to the existence of localized 4*f* moments on the Eu^{2+} site [220,221]. Similar to $SrTiO_3$, strain can be used to soften the soft mode and drive it to a ferroelectric instability. In contrast to $SrTiO_3$, which is diamagnetic, the permittivity of bulk $EuTiO_3$ is strongly coupled with its magnetism, showing an abrupt decrease in dielectric constant at the onset of the antiferromagnetic Eu^{2+} ordering [222]. This indicates that the soft mode frequency hardens when the spins order antiferromagnetically; conversely it will soften if the spins order ferromagnetically. This extra interaction provides the coupling favoring a simultaneously ferroelectric and ferromagnetic ground state under sufficient strain in $EuTiO_3$.

Although testing this prediction seems straightforward, the groups who first tested it ran into an unforeseen complication: no matter what substrate they deposited the $EuTiO_3$ on it was ferromagnetic! With its identical lattice constant (both are 3.905 Å at room temperature), $SrTiO_3$ is an obvious substrate for the growth of unstrained epitaxial $EuTiO_3$ films. Surprisingly, as-grown $EuTiO_{3-\delta}$ thin films synthesized by PLD on (001) $SrTiO_3$ substrates exhibit expanded out-of-plane spacings (0.4–2% longer than bulk $EuTiO_3$) [223–226] and are *ferromagnetic* with a Curie temperature of about 5 K [224,225]. Further, the negligible (<0.5%) variation in the cubic lattice constant of oxygen deficient $EuTiO_{3-\delta}$ over its wide single phase field [227,228], up to the $EuTiO_{2.5}$ limit [227] of the perovskite $EuTiO_{3-\delta}$ structure, is insufficient to explain the 2% variation in out-of-plane lattice spacings observed in epitaxial $EuTiO_{3-\delta}$ films grown on (001) $SrTiO_3$ by PLD [224–226].

One possibility is that the ferromagnetism observed in epitaxial $EuTiO_3$ films prepared by PLD on $SrTiO_3$ arises from extrinsic effects. Extrinsic effects are known to occur in thin films, particularly for deposition technologies involving energetic species, which can induce defects. For example, some homoepitaxial $SrTiO_3$ films grown by PLD have been reported to be ferroelectric [229] in striking contrast to the intrinsic properties of $SrTiO_3$, which is not ferroelectric at any temperature [230]. Homoepitaxial $SrTiO_3$ films grown by PLD are also known to exhibit lattice spacings that deviate significantly from the $SrTiO_3$ substrates they are grown on [154,156,157], although $SrTiO_{3-\delta}$ itself exhibits negligible variation in its cubic lattice constant up to the $SrTiO_{2.5}$ limit [231,232] of the perovskite $SrTiO_{3-\delta}$ structure in bulk. The sensitivity of $EuTiO_3$ that makes it an appropriate material to transmute via strain into a multiferroic also makes it quite sensitive to defects. To overcome this issue and see the intrinsic effect of strain on $EuTiO_3$, a more delicate deposition technique was needed.

Until very recently, only $SrTiO_3$ films grown by MBE [233] exhibited bulk behavior and none of the unusual effects reported in $SrTiO_3$ films grown by PLD [154,156,157,229], but recent PLD studies have demonstrated bulk-like structure, dielectric response, and thermal properties through careful control of film composition in PLD growth [234]. Indeed unstrained, stoichiometric $EuTiO_3$ thin films grown by MBE on (001) $SrTiO_3$ have the same lattice constant as bulk $EuTiO_3$ and are antiferromagnetic [235]. $EuTiO_3$ films deposited by MBE led to the results shown in Fig. 5 and, in agreement with theory, produced the strongest multiferroic material known today [59].

3.2.2. Strain-induced effects in $BiFeO_3$

No other multiferroic thin-film material has received as much attention as $BiFeO_3$ which is essentially the only single-phase

multiferroic that simultaneously possesses both magnetic and ferroelectric order at and above room temperature. Although first studied in the late 1950s [236] and extensively developed during the subsequent decades, $BiFeO_3$ has invigorated the scientific community in the last decade. $BiFeO_3$ has a rhombohedral unit cell characterized by two distorted perovskite blocks connected along their body diagonal ($\langle 1\,1\,1\rangle_p$) where the two oxygen octahedra of the two cells are rotated clockwise and counterclockwise around the $\langle 1\,1\,1\rangle$ by ±13.8(3)° and the Fe-ion is shifted by 0.135 Å along the same axis [237]. $BiFeO_3$ is a robust ferroelectric (saturation polarization of 90–100 μC/cm^2, $T_C \sim 1103$ K) [11,238] and antiferromagnetic (G-type, Néel temperature ~673 K [239]) with a cycloidal spin structure with a period of ~620 Å [240]. The symmetry also permits a small canting of the moments in the structure resulting in a weak canted ferromagnetic moment of the Dzyaloshinskii–Moriya type [241,242].

Spurred on by a 2003 paper focusing on the growth and properties of thin films of $BiFeO_3$ [11] dramatic advances in the study and understanding of this material have occurred. Here we will recap advances in the last few years. Thin-film samples of $BiFeO_3$ has been grown by just about every conceivable thin-film growth technique on a wide range of substrates including traditional perovskite oxide substrates (with lattice parameters ranging from 3.71 to 4.01 Å, covering a range from 7% compressive strain to 1.3% tensile strain) as well as Si and GaN. The ability to synthesize and manipulate these materials as thin films has provided a fine-level of control of properties. This includes the ability to change the easy direction of magnetization in $BiFeO_3$ thin films by changing the sign of thin-film strain [243] and controlling domain structures in $BiFeO_3$. By balancing elastic and electrostatic energy considerations, researchers have demonstrated 1-dimensional nanoscale domain arrays [244] (which possess excellent room temperature ferroelectric properties) [245], deterministic control of polarization variants [246], and generation of equilibrium domain structures [247] (Fig. 6) that had been predicted nearly a decade earlier [248].

At the same time, the availability of high-quality thin-film samples of these materials has made possible a range of exciting observations. Researchers have observed a systematic dependence of the ferroelectric domain structure in $BiFeO_3$ films as a function of the growth rate [249] with stripe-like and mosaic-like varieties possessing different types and densities of domain walls. The presence of certain types of domain walls has, in turn, been related to the overall magnetic moment observed in $BiFeO_3$ and to exchange bias between $BiFeO_3$ and metallic ferromagnets [249]. Taking this idea one step further, Daraktchiev et al. [250,251] used a thermodynamic (Landau-type) model to examine whether the domain walls in $BiFeO_3$ can be magnetic and, if so, to what extent they might contribute to the observed enhancement of magnetization. They found that when the polarization gores from $+P$ to $-P$, it is energetically more favorable for the domain wall energy trajectory not to go through the center of the landscape ($P = 0$, $M = 0$), but to take a diversion through the saddle points at $M_0 \neq 0$, thus giving rise to a finite magnetization. Thus it is possible for a net magnetization to appear in the middle of ferroelectric walls even when the domains themselves are not ferromagnetic. Recent magnetotransport studies by He et al. [252] have demonstrated that certain types of domain walls (i.e., 109° walls) can exhibit strong temperature- and magnetic field-dependent magnetoresistance (as large as 60%) which is thought to be the result of local symmetry breaking at domain walls and the formation of magnetic moments (Fig. 7). This work builds off of prior work [249] that demonstrated that samples possessing 109° domain walls show significantly enhanced circular dichroism that is consistent with collective magnetic correlations, while samples with only 71° domain walls show no measurable circular dichroism.

At the same time, detailed scanning probe-based studies of domain walls in $BiFeO_3$ have resulted in the discovery of unanticipated room temperature electronic conductivity at domain walls (Fig. 8) [253]. From combined local conductivity measurements, electron microscopy analysis, and density functional theory calculations it has been suggested that an increased carrier density (arising from the formation of an electrostatic potential step at the wall) and a decrease in the band gap within the wall and corresponding reduction in band offset with the scanning-probe tip could be responsible for the phenomenon. Such concepts are consistent with calculation of a similar potential step at 90° domain walls in $PbTiO_3$ [254] that would enhance the electrical conductivity by causing carriers in the material to accumulate at the domain wall to screen the polarization discontinuity. It is likely that that both effects (which arise for similar reasons) may be acting simultaneously, since they are not mutually exclusive. Recently additional effects from oxygen vacancies have been reported in domain walls in $BiFeO_3$ [255], tunable conductivity and memresistor-like function has been observed at such domain walls [256], and conducting domain wall features in other ferroelectrics such as $PbZr_{0.2}Ti_{0.8}O_3$ have been observed [257].

As we have noted, epitaxy presents a powerful pathway to control the phase stability and electronic properties in thin-film systems [258]. The $BiFeO_3$ system presents a fascinatingly complex strain-driven structural evolution. Although the structure of $BiFeO_3$ had been studied for many years [259–261], in 2005 the structural stability of the parent phase had come into question [262,263]. This was followed, in turn, by a number of thin-film studies reporting that a tetragonally-distorted phase (derived from a structure with $P4mm$ symmetry, $a \sim 3.665$ Å, and $c \sim 4.655$ Å) with a large spontaneous polarization may be possible [56,262,264]. In 2009, so-called mixed-phase thin films possessing tetragonal- and rhombohedral-like phases in complex stripe-like structures (and large electromechanical responses) [60] dramatically changed the study of structures in $BiFeO_3$. It was found that the rhombohedral bulk crystal structure of the parent phase can be progressively distorted into a variety of unit cell structures through epitaxial strain. *Ab initio* calculations of the role of epitaxial strain clearly demonstrate how it can be used to drive a strain-induced structural change in $BiFeO_3$ (Fig. 9a and b). These calculations suggest that at a certain value of epitaxial strain, in the absence of misfit accommodation through dislocation formation, the structure of $BiFeO_3$ morphs from the distorted rhombohedral parent phase to a tetragonal-like (actually monoclinic) structure that is characterized by a large c/a ratio of ~1.26. Direct atomic resolution images of the two phases (Fig. 9c and d) clearly show the difference in the crystal structures.

Much recent attention has been given to what happens when films are grown at intermediate strain levels (e.g., ~4.5% compressive strain, corresponding to growth on $LaAlO_3$ substrates). It has been observed that the result is a nanoscale mixed-phase structure (Fig. 9e and f). Fig. 9g is an atomic resolution TEM image of the interface between these two phases and reveals one of the most provocative aspects of these structures. Although there is a large "formal" lattice mismatch between the two phases, the interface appears to be coherent, i.e., it shows no indication for the formation of interphase dislocations. Indeed, this mismatch appears to be accommodated by the gradual deformation of the structure between different phases.

Considerable detail has emerged concerning the symmetry of these phases including the fact that the so-called tetragonal-like phase is actually monoclinically distorted (possessing *Cc*, *Cm*, *Pm*, *or Pc* symmetry) [58,62,265,266]. Other techniques such as second harmonic generation have been used to probe these different structures as well [267]. Recent reports [268] have also investigated the driving force for the formation of these so-called

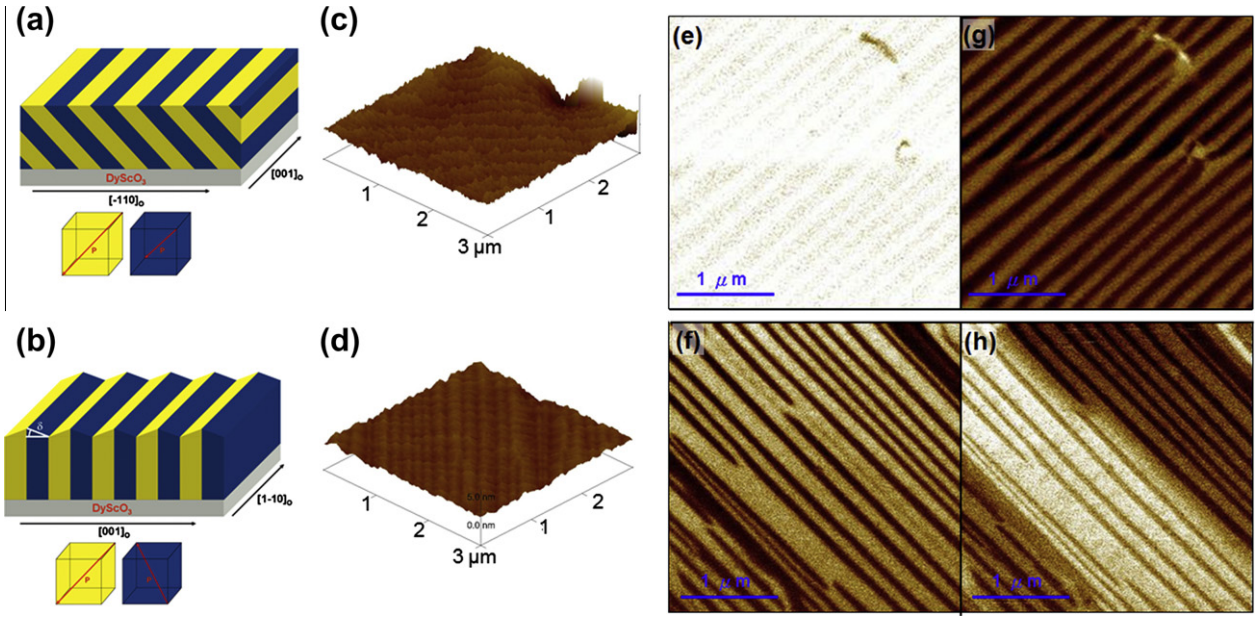

Fig. 6. Ordered arrays of ferroelectric domains and domain walls. (a) and (b) Schematics of equilibrium structure of an ordered array of 71° and 109° domain walls, respectively. (c) and (d) Surface topography as measured by AFM of 71° and 109° domain walls samples, respectively. Out-of-plane (e) and (f) as well as in-plane (g) and (h) PFM images for samples possessing ordered arrays of 71° and 109° domain walls. (Adapted from Ref. [248]).

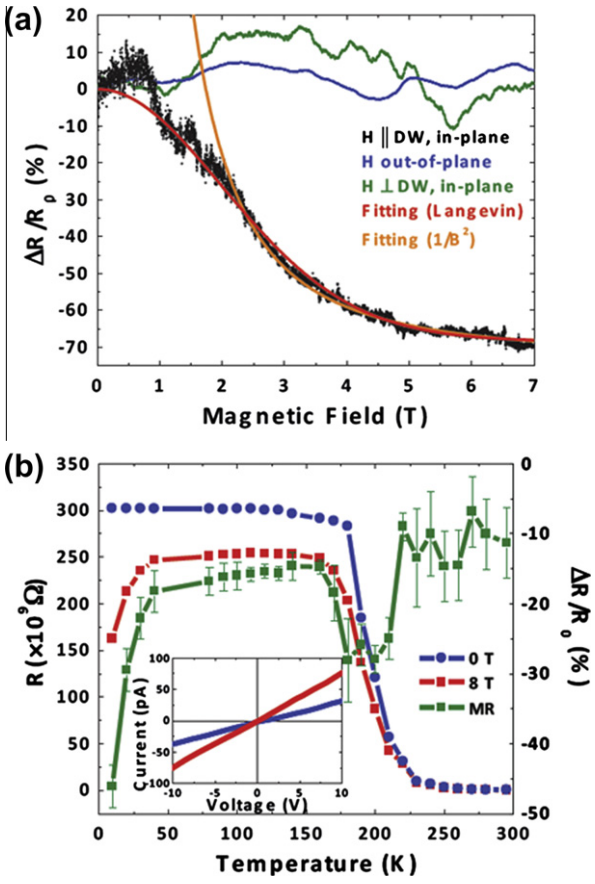

Fig. 7. Magnetotransport study of 109° domain walls in $BiFeO_3$ films. (a) Anisotropic magnetoresistance measured at 10 K in various directions of external magnetic field. (b) Resistance-temperature curves at two different external magnetic fields, 8 T (red) and 0 T (blue) and the corresponding magnetoresistance (green). (Adapted from Ref. [252]).

mixed-phase structures and have revealed a complex temperature- and thickness-dependent evolution of phases in the $BiFeO_3/LaAlO_3$ system. A thickness-dependent transformation from the monoclinically distorted tetragonal-like phase to a complex mixed-phase structure likely occurs as the consequence of a strain-induced spinodal instability. Additionally, a breakdown of this strain-stabilized metastable mixed-phase structure to non-epitaxial microcrystals of the parent rhombohedral structure of $BiFeO_3$ is observed to occur at a critical thickness of ~300 nm. Other reports have demonstrated routes to stabilize these structures [269]. At the same time, electric field dependent studies to these mixed-phase structures has also revealed the capacity for large electromechanical responses (as large as 4–5%). *In situ* TEM studies coupled with nanoscale electrical and mechanical probing suggest that these large strains result from the motion of boundaries between different phases [270]. Despite this work, a thorough understanding of the complex structure of these phase boundaries in $BiFeO_3$ remained incomplete until 2011.

A perspective by Scott [271] discussed the symmetry and thermodynamics of the phase transition between these two phases as well as a number of other model iso-symmetric phase transitions in other crystal systems. Soon after, a very detailed thermodynamic and elastic domain theory analysis of the mixed-phase structure was completed by Ouyang et al. [272]. In that treatment, a balance of interdomain elastic, electrostatic, and interface energies was analyzed and compared to provide an anticipated low-energy structural configuration. Subsequent studies by Damodaran et al. [273] helped uniquely identify and examine the numerous phases present at these phase boundaries and resulted in the discovery of an intermediate monoclinic phase in addition to the previously observed rhombohedral- and tetragonal-like phases. Further analysis determined that the so-called mixed-phase regions of these films were not mixtures of the parent rhombohedral- and tetragonal-like phases, but were mixtures of highly-distorted monoclinic phases with no evidence for the presence of the rhombohedral-like parent phase. This work helped confirm the mechanism for the enhanced electromechanical response and provide a model for how these phases interact at the nanoscale to produce large surface strains (Fig. 10). By undertaking local electric field switching studies and navigating the hysteretic nature of

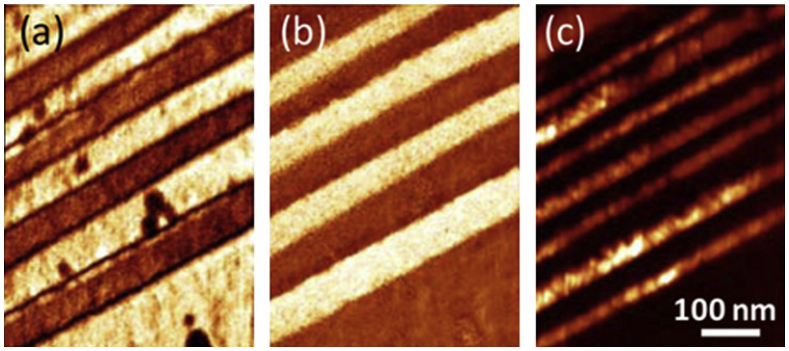

Fig. 8. Piezoresponse force microscopy (a) amplitude and (b) phase images of a 109° stripe domains in a $BiFeO_3$ sample. (c) Simultaneously acquired conducting-AFM image of the same area showing that each 109° domain wall is electrically conductive. (Adapted from Ref. [255]).

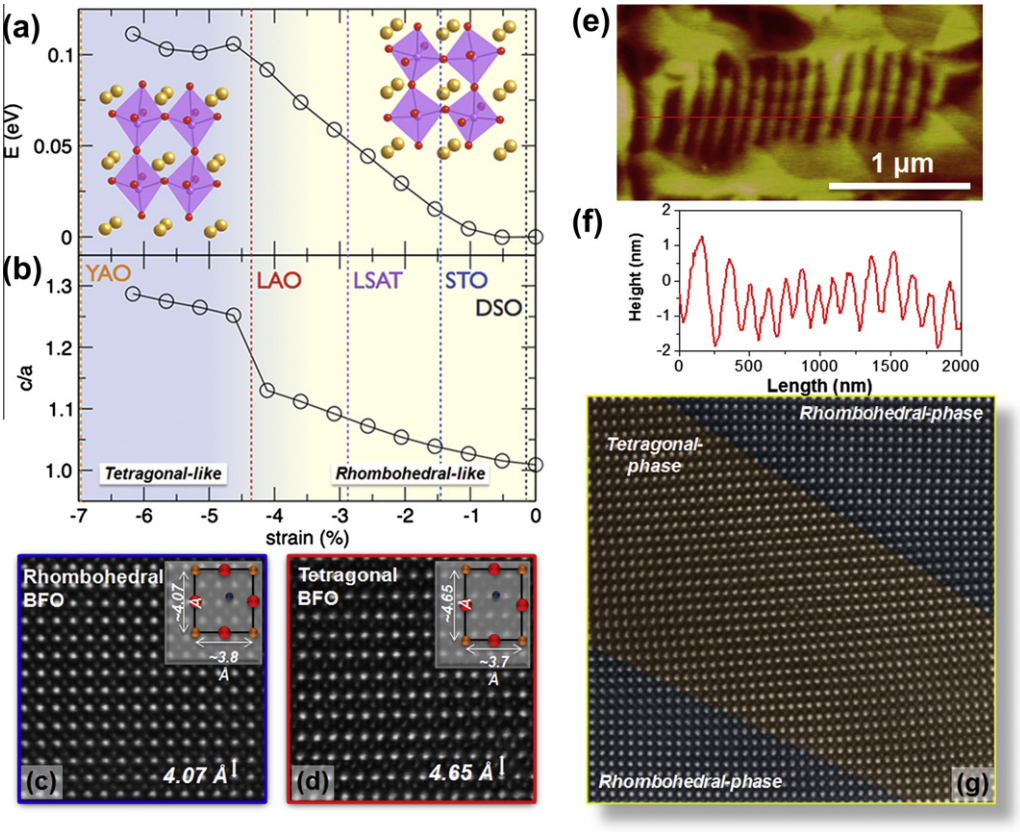

Fig. 9. Strain-induced phase complexity in $BiFeO_3$. First-principle calculations provide information on the strain evolution of (a) the overall energy of the system and (b) the *c*/*a* lattice parameter ratio. High-resolution transmission electron microscopy (HRTEM) reveals the presence of two phase (c) a monoclinic version of the bulk rhombohedral phase and a (d) high-distorted monoclinic version of a tetragonal structure. These complex phase boundaries manifest themselves on the surface of the sample as imaged via (e) atomic force microscopy and these features correspond to dramatic surface height changes as shown from (f) the line trace. (g) HRTEM imaging of boundaries shows a smooth transition between phases. (Adapted from Ref. [60]).

electric field response in this material, a number of important features were revealed: (1) the large surface strains (4–5%) occur any time the material transforms form a mixed-phase structure to the highly-distorted monoclinic phase, (2) transformations between these two states are reversible, and (3) there are numerous pathways to achieve large electromechanical responses in these materials – including ones that do not need ferroelectric switching. The key appears to be the ability to transform between the different phases through a diffusion-less phase transition (akin to a martensitic phase). Similar discussions of the nature of the electric field driven phase transformation have also been reported [274]. This report additionally included single-point spectroscopic studies that suggest that the tetragonal-like to rhombohedral-like transition is activated at a lower voltage compared to a ferroelectric switching of the tetragonal-like phase and the formation of complex rosette domain structures that have implications for future devices.

A number of additional studies on these strain-induced phases have been reported in recent months. This includes considerable discussion on magnetic and magnetoelectric properties of these materials. Researchers have investigated the emergence of an enhanced spontaneous magnetization in the so-called mixed phase structures [275]. Using X-ray magnetic circular dichroism-based photoemission electron microscopy coupled with macroscopic

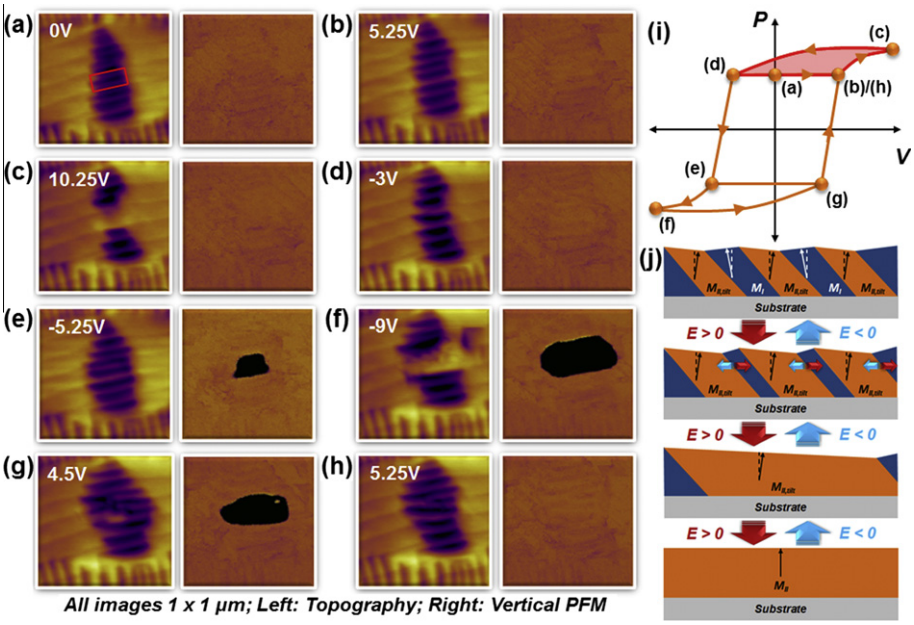

Fig. 10. AFM image (left) and vertical PFM image (right) of 100 nm $BiFeO_3/La_{0.5}Sr_{0.5}CoO_3/LaAlO_3$ (0 0 1) in the (A) as-grown state and after being poled in the box at (B) 5.25 V, (C) 10.25 V, (D) −3 V, (E) −5.25 V, (F) −9 V, (G) 4.5 V, and (H) 5.25 V. (All images are 1 × 1 μm.) (I) A schematic hysteresis loop with letters corresponding to the images in (A–H) shows the multiple pathways to enhanced electromechanical response. (J) Illustration of the proposed mechanism for the large electromechanical response without the need for ferroelectric switching. (Adapted from Ref. [273]).

magnetic measurements, the researchers found that the spontaneous magnetization of the new intermediate monoclinic phase is significantly enhanced above the expected moment of the parent phase as a consequence of a piezomagnetic coupling to the adjacent tetragonal-like phase. Soon after this report, researchers suggested that the magnetic Néel temperature of the strained $BiFeO_3$ is suppressed to around room temperature and that the ferroelectric state undergoes a first-order transition to another ferroelectric state simultaneously with the magnetic transition [276]. This has strong implications for room temperature magnetoelectric applications. This observation, builds off of a detailed neutron scattering study of a nearly phase-pure film of the highly distorted tetragonal-like phase which confirms antiferromagnetism with largely G-type character and a T_N = 324 K, a minority magnetic phase with C-type character, and suggests that the co-existence of the two magnetic phases and the difference in ordering temperatures from the bulk phase can be explained through simple Fe–O–Fe bond distance considerations [277]. At the same time, other reports suggest the possibility of a reversible temperature-induced phase transition at about 373 K in the highly distorted tetragonal-like phase as studied by temperature-dependent Raman measurements [278]. Similar results have been reported from temperature dependent X-ray diffraction studies that reveal a structural phase transition at ~373 K between two monoclinic structures [279]. Finally there are reports of a concomitant structural and ferroelectric transformation around 360 K based on temperature-dependent Raman studies. This work suggests that the low-energy phonon modes related to the FeO_6 octahedron tilting show anomalous behavior upon cooling through this temperature – including an increase of intensity by one order of magnitude and the appearance of a dozen new modes [280]. Truly this is an exciting and fast-moving field of study today. Such electric field and temperature induced changes of the phase admixture is also reminiscent of the CMR manganites or the relaxor ferroelectrics and is accompanied by large electromechanical strains, but there appears to be much more to these mixed-phase structures. Such structural softness in regular magnetoelectric multiferroics—i.e., tuning the materials to make their structure strongly reactive to applied fields—makes it possible to obtain very large magnetoelectric effects [281].

4. Future directions and conclusions

The purpose of this review was to highlight some of the exciting new developments in the field of thin-film multiferroics and magnetoelectrics. This field remains highly active and new developments are occurring at a rapid pace that shine light onto the complexities inherent to these materials. Dramatic advances in thin-film growth technology and know-how has been a key enabler fueling these discoveries as has been demonstrated here. As we look forward at the field of thin film multiferroics there are numerous opportunities for development.

Thin film techniques have had a major impact on *perovskite* multiferroics with $BiFeO_3$ being the prime example. The discoveries that $BiFeO_3$ has a huge spontaneous polarization and that it can be morphed into various polymorphs and polymorphic mixtures were all made using epitaxial films. Yet there are many other fascinating multiferroic oxides—$YMnO_3$, $LuFe_2O_4$, and hexaferrites like $Sr_3Co_2Fe_{24}O_{41}$ [282] to name a few—that are comparatively ignored by the thin film community and are the focus of the single crystal multiferroic community. Why is this? We think the issue is the lack of suitable substrates for these latter structures that is the main roadblock; removing this barrier is an opportunity for the future. Once high quality films can be made, the technological advantage of a thin-film geometry to lower switching voltages and enable integration into more sophisticated heterostructures, as is now common for $BiFeO_3$, can be exploited.

Imagine the opportunities that substrates for the non-perovskite multiferroic systems would bring. Substrates for $YMnO_3$ would enable more variants of hexagonal manganite multiferroics to be constructed. These variants include not only known materials, but more interestingly enhanced variants of known materials using strain engineering, metastable multiferroic polymorphs (e.g., $LuFeO_3$ that is isostructural to $YMnO_3$ rather than its stable centrosymmetric perovskite form) [283,284] by utilizing lattice

misfit strain energies and interfacial energies to favor the desired metastable phase over the equilibrium phase (epitaxial stabilization) [285–288], or the prospect of interfacial multiferroicity that has been predicted to emerge in superlattices between centrosymmetric components [289]. Similarly substrates with the $LiNbO_3$ structure would enable the growth of the $LiNbO_3$-polymorph of $FeTiO_3$ and related multiferroics [290,291]. A range of appropriate substrates, like the range of substrates available for perovskites shown in Fig. 3, for each multiferroic system of interest would allow the powerful toolbox of the epitaxial engineer to be freely applied to a much larger set of multiferroic building blocks. These tools include strain engineering, epitaxial stabilization, polarization engineering [145,292], and superlattice formation.

Looking forward there are a number of challenges that face the multiferroics/magnetoelectrics community. First, although excitement has been riding high for nearly 30 years about the promise of complex, functional oxide materials such as high-temperature superconductivity, ferroelectrics, colossal magnetoresistance materials, and now multiferroics, transitioning these fundamental materials discoveries into real products has remained difficult. Although there are some exciting success stories, the complexity of these materials is compounded by the many steps involved in fabrication scalable devices. With current funding opportunities from the United States government meant to address manufacturing and the process of scaling materials from basic science to product, the outlook will hopefully be very positive.

Nonetheless, one of the biggest challenges facing the field of multiferroics today is the need for room temperature function. Thus, it is essential that the field works to include both thin-film heterostructure and bulk synthesis methods and broadens the search for new candidate multiferroics. This additionally relies on the interplay of theoretical approaches, advanced growth techniques, and characterization. As this mini-series of articles highlights, these concepts have found a home in multiferroics. As the field progresses, it is expected that thin films with appropriately designed and controlled heteroepitaxial constraints (such as strain, clamping, and possibly surface termination) are important variables that will provide additional control of properties and a challenging set of interdisciplinary condensed matter research problems.

To address these challenges, the community will need to attack a number of limitations. One example of an area ripe for development is the synthesis of substrates that would enable production and fine-level epitaxial control of non-perovskite multiferroic systems (e.g., $LuFe_2O_4$, $YMnO_3$, hexaferrites such as $Sr_3Co_2Fe_{24}O_{41}$ [282], and materials with the $LiNbO_3$ structure such as the $LiNbO_3$-polymorph of $FeTiO_3$ and related multiferroics [290,291]). At the same time, taking the approach of an epitaxial engineer, it would be interesting to examine new routes to develop additional variants of hexagonal ferrites using a superlattice layering approach – in essence asking if we can extend our unit-cell level control beyond basic perovskite structures – as opposed to the atomic substitution approach of a solid state chemist. Such advances would allow the tricks-of-the-trade of the epitaxial engineer including strain engineering, epitaxial stabilization of metastable multiferroic polymorphs (e.g., $LuFeO_3$ that is isostructural to $YMnO_3$ rather than a its stable centrosymmetric perovskite form) [283,284], and superlattice formation to be applied to these exciting multiferroics.

Yet another pathway to overcome the limitations in room-temperature functionality is to move to composite heterostructures that make use of exchange biased structure. One possible solution is to utilize heterostructures of existing multiferroic materials and to take advantage of two different types of coupling in materials – *intrinsic* magnetoelectric coupling as demonstrated in single-phase multiferroic materials which will allow for electrical control of antiferromagnetism (as in the case of $BiFeO_3$) and the *extrinsic* exchange coupling between ferromagnetic and antiferromagnetic materials – to create new functionalities in materials. By utilizing these different types of coupling we can then effectively couple ferroelectric and ferromagnetic order at room temperature and create an alternative pathway to electrical control of ferromagnetism Among the earliest work in this area was a study of heterostructures of the soft ferromagnet permalloy on $YMnO_3$ [293] that demonstrated that a multiferroic layer could be used as an antiferromagnetic pinning layer that gives rise to exchange bias and enhanced coercivity. Subsequently Marti et al. [294] reported the observation of exchange bias in all-oxide heterostructure of the ferromagnet $SrRuO_3$ and the antiferromagnetic, multiferroic $YMnO_3$ (albeit only at very low temperatures). Around the same time, studies using $BiFeO_3$ as the multiferroic, antiferromagnetic layer by Dho et al. [295] showed the existence of exchange bias in spin-valve structures based on permalloy and $BiFeO_3$ at room temperature and Béa et al. [296] extended this idea to demonstrate how $BiFeO_3$ films could be used in first generation spintronics devices. In turn, Martin et al. [297] reported the growth and characterization of exchange bias and spin valve heterostructures based on $Co_{0.9}Fe_{0.1}$/$BiFeO_3$ heterostructures on Si substrates. These initial studies established, was that exchange bias with antiferromagnetic multiferroics was possible in a static manner, but these studies had not yet demonstrated dynamic control of exchange coupling in these systems.

In this spirit, Borisov et al. [298] reported that they could affect changes on the exchange bias field in Cr_2O_3 (1 1 1)/$(Co/Pt)_3$ heterostructures by using the magnetoelectric nature of the substrate (Cr_2O_3) and a series of different cooling treatments with applied electric and magnetic fields. Dynamic switching of the exchange bias field with an applied electric field, however, remained elusive until a report by Laukhin et al. [299] focusing on $YMnO_3$ at 2 K. Studies focusing again on $BiFeO_3$-based heterostructures illustrated the importance of domains and domain walls in controlling the magnetic coupling in these structures [249,300]. In addition to identifying the importance of 109° domain walls in creating exchange bias, this work served as the foundation for the observation of room temperature electric field control of ferromagnetic domain structures. Using high quality $Co_{0.9}Fe_{0.1}/BiFeO_3/SrRuO_3/SrTiO_3$ (0 0 1) heterostructures, researchers have been able to deterministically change the direction of ferromagnetic domains in the $Co_{0.9}Fe_{0.1}$ by 90° upon application an applied electric field to the $BiFeO_3$ [301]. Recently attention has turned back Cr_2O_3 and exciting work in electric field control of ferromagnetism. Using a combination of modern thin film growth techniques, magnetometry, spin-polarized photoemission spectroscopy, symmetry arguments, and first-principles He et al. [302] studied Pd/Co multilayers deposited on (0 0 0 1) surface of the antiferromagnet Cr_2O_3 and demonstrated reversible, room temperature isothermal switching of the exchange bias field from positive to negative values by reversing the electric field under a constant magnetic field. Still further, all-oxide interfaces have been examined including $La_{0.7}Sr_{0.3}MnO_3$–$BiFeO_3$ epitaxial heterostructures where the formation of a novel ferromagnetic state in the antiferromagnet $BiFeO_3$ at the interface was reported [303].

In the end, as we look back at the development of complex oxide research we see a series of exciting discoveries from high T_C superconductivity to multiferroism have propelled the greater field of oxides to the forefront of condensed matter physics. The diverse functionality of oxide materials means that this breakthrough could drive the field towards many of the major scientific questions that face us today – from energy, to medicine, to communications, and beyond.

Acknowledgements

L.W.M. acknowledges the support of the Army Research Office under Grant W911NF-10-1-0482 and the Samsung Electronics

Co., Ltd. under Grant 919 Samsung 2010-06795. D.G.S. acknowledges the support of the U.S. Department of Energy, Office of Basic Energy Sciences, Division of Materials Sciences and Engineering under Award #DE-SC0002334. Both authors have benefitted from the numerous collaborations, within programs at UIUC, UC Berkeley, LBNL, Cornell, Penn State, as well as numerous other valued collaborators around the world.

References

[2] He Q, Arenholz E, Scholl A, Chu YH, Ramesh R. Nanoscale characterization of emergent phenomena in multiferroics. Current Opin Solid State Mater Sci 2011; YY, yyyy.
[3] Rao CNR, Raveau B. Transition metal oxides. New York: Wiley-VCH; 1998.
[4] Norton D. Synthesis and properties of epitaxial electronic oxide thin-film materials. Mater Sci Eng R 2004;43:139–247.
[5] Smyth DM. The defect chemistry of metal oxides. New York: Oxford University Press; 2000.
[6] Schmid H. Multi-ferroic magnetoelectrics. Ferroelectrics 1994;162:317–38.
[7] Fiebig M. Revival of the magnetoelectric effect. J Phys D 2005;38:R123–152.
[8] Eerenstein W, Mathur ND, Scott JF. Multiferroic and magnetoelectric materials. Nature 2006;442:759–65.
[9] Hill NA. Why are there so few magnetic ferroelectrics. J Phys Chem B 2000;104:6694–709.
[10] Khomskii D. Classifying multiferroics: mechanisms and effects. Physics 2009;2:20.
[11] Wang J, Neaton JB, Zheng H, Nagarajan V, Ogale SB, Liu B, et al. Epitaxial $BiFeO_3$ mutliferroic thin film heterostructures. Science 2003;299:1719–22.
[12] van Aken BB, Palstra TTM, Filippetti A, Spaldin NA. The origin of ferroelectricity in magnetoelectric $YMnO_3$. Nature Mater 2004;3:164–70.
[13] Ikeda N, Ohsumi H, Ohwada K, Ishii K, Inami T, Kakurai K, et al. Ferroelectricity from iron valence ordering in the charge-frustrated system $LuFe2O_4$. Nature 2005;436:1136–8.
[14] Kimura T, Goto T, Shintani H, Ishizaka K, Arima T, Tokura Y. Magnetic control of ferroelectric polarization. Nature 2003;426:55–8.
[15] Hur N, Park S, Sharma PA, Ahn JS, Guha S, Cheong SW. Electric polarization reversal and memory in a multiferroic material induced by magnetic fields. Nature 2004;429:392–5.
[16] Nan CW, Bichurin MI, Dong S, Viehland D, Srinivasan G. Multiferroic magnetoelectric composites: historical perspective, status, and future directions. J Appl Phys 2008;103:031101.
[17] Wang Y, Hu J, Nan CW. Multiferroic magnetoelectric composite nanostructures. NPG Asia Mater 2010;2:61–8.
[18] Ma J, Hu J, Li Z, Nan CW. Recent progress in multiferroic magnetoelectric composites: from bulk to thin films. Adv Mater 2011;23:1062–87.
[19] van Suchtelen J. Product properties: a new application of composite materials. Philips Res Rep 1972;27:28–37.
[20] van Run AMJG, Terrell DR, Scholing JH. An*in situ g* rown eutectic magnetoelectric composite material: part 2 physical properties. J Mater Sci 1974;9:1710–4.
[21] Bracke LPM, van Vliet RG. A broadband magneto-electric transducer using a composite material. Int J Electron 1981;51:255–62.
[22] van den Boomgaard J, Terrell DR, Born RAJ. An*in situ* grown eutectic magnetoelectric composite material. J Mater Sci 1974;9:1705–9.
[23] Newnham RE, Skinner DP, Cross LE. Connectivity and piezoelectric-pyroelectric composites. Mater Res Bull 1978;13:525–36.
[24] Avellaneda M, Harshe G. Magnetoelectric effect in piezoelectric/magnetoresistive multilayer (2-2) composites. J Int Mat Syst Str 1994;5:501–13.
[25] Ryu J, Priya S, Carazo AV, Uchino K, Kim H. Effect of the magnetostrictive layer on magnetoelectric properties in PZT/Terfenol-D laminate composites. J Am Ceram Soc 2001;84:2905–8.
[26] Ryu S, Park JH, Jang HM. Magnetoelectric coupling of [00l]-oriented $Pb(Zr_{0.4}Ti_{0.6})O_3$–$Ni_{0.8}Zn_{0.2}Fe_2O_4$ multilayered thin films. Appl Phys Lett 2007;91:142910.
[27] Ryu J, Carazo AV, Uchino K, Kim H. Piezoelectric and magnetoelectric properties of lead zirconate titanate/Ni-ferrite particulate composites. J Electroceram 2001;7:17–24.
[28] Srinivasan G, Rasmussen ET, Gallegos J, Srinivasan R. Magnetoelectric bilayer and multilayer structures of magnetostrictive and piezoelectric oxides. Phys Rev B 2001;64:214408.
[29] Srinivasan G, Rasmussen ET, Levin BJ, Hayes R. Magnetoelectric effects in bilayers and multilayers of magnetostrictive and piezoelectric perovskite oxides. Phys Rev B 2002;65:134402.
[30] Srinivasan G, Rasmussen ET, Bush AA, Kamentsev KE. Structural an magnetoelectric properties of MFe_2O_4 -PZT (M = Ni, Co) and $La_x(Ca, Sr)_{1-x}MnO_3$ -PZT multilayer composites. Appl Phys A 2004;78:721–8.
[31] Ryu J, Priya S, Uchino K, Kim HE. Magnetoelectric effect in composites of magnetostrictive and piezoelectric materials. J Electroceram 2002;8:107–19.
[32] Bichurin MI, Petrov VM, Srinivasan G. Theory of low-frequency magnetoelectric coupling in magnetostrictive-piezoelectric bilayers. Phys Rev B 2003;68:054402.
[33] Zheng H, Wang J, Lofland SE, Ma Z, Mohaddes-Ardabili L, Zhao T, et al. Multiferroic $BaTiO_3$ -$CoFe_2O_4$ nanostructures. Science 2004;303:661–3.
[34] Zheng H, Zhan Q, Zavaliche F, Sherburne M, Straub F, Cruz MP, et al. Controlling self-assembled perovskite-spinel nanostructures. Nanoletter 2006;7:1401–7.
[35] Li J, Levin I, Slutsker J, Provenzano V, Schenck PK, Ramesh R, et al. Self-assembled multiferroic nanostructures in the $CoFe_2O_4$ -$PbTiO_3$ system. Appl Phys Lett 2005;87:072909.
[36] Wan JG, Wang XW, Wu YJ, Zeng M, Wang Y, Jiang H, et al. Magnetoelectric $CoFe_2O_4$ -$Pb(Zr,Ti)O_3$ composite thin films derived by a sol-gel process. Appl Phys Lett 2005;86:122501.
[37] Ren S, Wuttig M. Spinodally synthesized magnetoelectric. Appl Phys Lett 2007;91:083501.
[38] Zhan Q, Yu R, Crane SP, Zheng H, Kisielowski C, Ramesh R. Structure and interface chemistry of perovskite-spinel nanocomposite thin films. Appl Phys Lett 2006;89:172902.
[39] Murakami M, Fujino S, Lim SH, Salamanca-Riba LG, Wuttig M, Takeuchi I, et al. Microstructure and phase control in Bi-Fe-O multiferroic nanocomposite thin films. Appl Phys Lett 2006;88:112505.
[40] Schlom DG, Chen LQ, Eom CB, Rabe KM, Streiffer SK, Triscone JM. Strain tuning of ferroelectric thin films. Ann Rev Mater Res 2007;37:589–626.
[41] Schlom DG, Haeni JH, Lettieri J, Theis CD, Tian W, Jiang JC, et al. Oxide nano-engineering using MBE. Mater Sci Eng B 2001;87:282–91.
[42] Lindh AE. Physics 1946 Percy Williams Bridgman. In: Nobel lectures in physics 1942–1962. Singapore: World Scientific; 1998. p. 49–52.
[43] Lock JM. Penetration of magnetic fields into superconductors III. Measurements on thin films of tin, lead and indium. Proc Royal Soc Lond 1951;A208:391–408.
[44] Forsbergh Jr PW. Effect of a two-dimensional pressure on the Curie point of barium titanate. Phys Rev 1954;93:686–92.
[45] Gumbsch P, Taeri-Baghbadrani S, Brunner D, Sigle W, Rühle M. Plasticity and an inverse brittle-to-ductile transition in strontium titanate. Phys Rev Lett 2001;87:085505.
[46] Nguyen LD, Brown AS, Thompson MA, Jelloian LM. 50-nm Self-aligned-gate pseudomorphic AlInAs/GaInAs high electron mobility transistors. IEEE Trans Electron Dev 1992;39:2007–14.
[47] Welser J, Hoyt JL, Gibbons JF. Electron mobility enhancement in strained-Si *n*-type metal-oxide-semiconductor field-effect transistors. IEEE Electron Dev Lett 1994;15:100–2.
[48] Sato H, Naito M. Increase in the superconducting transition temperature by anisotropic strain effect in (001) $La_{1.85}Sr_{0.15}CuO_4$ thin films on $LaSrAlO_4$ substrates. Physica C 1997;274:221–6.
[49] Bozovic I, Logvenov G, Belca I, Narimbetov B, Sveklo I. Epitaxial strain and superconductivity in $La_{2-x}Sr_xCuO_4$ thin films. Phys Rev Lett 2002;89:107001.
[50] Beach RS, Borchers JA, Matheny A, Erwin RW, Salamon MB, Everitt B, et al. Enhanced Curie temperatures and magnetoelastic domains in Dy/Lu superlattices and films. Phys Rev Lett 1993;70:3502–5.
[51] Gan Q, Rao RA, Eom CB, Garrett JL, Lee M. Direct measurement of strain effects on magnetic and electrical properties of epitaxial $SrRuO_3$ thin films. Appl Phys Lett 1998;72:978–80.
[52] Fuchs D, Arac E, Pinta C, Schuppler S, Schneider R. V. Löhneysen H. Tuning the magnetic properties of $LaCoO_3$ thin films by epitaxial strain. Phys Rev B 2008;77:014434.
[53] Haeni JH, Irvin P, Chang W, Uecker R, Reiche P, Li YL, et al. Room-temperature ferroelectricity in strained $SrTiO_3$. Nature 2004;430:758–61.
[54] Choi KJ, Biegalski M, Li YL, Sharan A, Schubert J, Uecker R, et al. Enhancement of ferroelectricity in strained $BaTiO_3$ thin films. Science 2004;306:1005–9.
[55] Warusawithana MP, Cen C, Sleasman CR, Woicik JC, Li YL, Fitting Kourkoutis L, et al. A ferroelectric oxide made directly on silicon. Science 2009;324:367–70.
[56] Béa H, Dupé B, Fusil S, Mattana R, Jacquet E, Warot-Fonrose B, et al. Evidence for room-temperature multiferroicity in a compound with giant axial ratio. Phys Rev Lett 2009;102:217603.
[57] Infante IC, Lisenkov S, Dupé B, Bibes M, Fusil S, Jacquet E, et al. Bridging multiferroic phase transitions by epitaxial strain in $BiFeO_3$. Phys Rev Lett 2010;105:057601.
[58] Chen Z, Luo Z, Huang C, Qi Y, Yang P, You L, et al. Low-symmetry monoclinic phases and polarization rotation path mediated by epitaxial strain in multiferroic $BiFeO_3$ thin films. Adv Funct Mater 2011;21:133–8.
[59] Lee JH, Fang L, Vlahos E, Ke X, Jung YW, Fitting Kourkoutis L, et al. A strong ferroelectric ferromagnet created by means of spin-phonon coupling. Nature 2010;466:954–8.
[60] Zeches RJ, Rossell MD, Zhang JX, Hatt AJ, He Q, Yang CH, et al. A strain-driven morphotrophic phase boundary in $BiFeO_3$. Science 2009;326:977–80.
[61] Chen P, Podraza NJ, Xu XS, Melville A, Vlahos E, Gopalan V, et al. Optical properties of quasi-tetragonal $BiFeO_3$ thin films. Appl Phys Lett 2010;96:131907.
[62] Christen H, Nam JH, Kim HS, Hatt AJ, Spaldin NA. Stress-induced R-M_A-M_C-T symmetry changes in $BiFeO_3$ films. Phys Rev B 2011;83:144107.
[63] Griffith AA. The phenomena of rupture and flow in solids. Philos Trans Roy Soc London Ser A 1920;221:163–98.
[64] Klokholm E, Matthews JW, Mayadas AF, Angilello J. Epitaxial strains and fracture in garnet films. In: Graham Jr CD, Rhyne JJ, editors. Magnetism and magnetic materials. New York: American Institute of Physics; 1972. p. 105–9.
[65] Freund LB, Suresh S. Thin film materials: stress, defect formation and surface evolution. Cambridge: Cambridge University Press; 2003. p. 60–83, 283–90, 396–416.

[66] Canedy CL, Li H, Alpay SP, Salamanca-Riba L, Roytburd AL, Ramesh R. Dielectric properties in heteroepitaxial $Ba_{0.6}Sr_{0.4}TiO_3$ thin films: effect of internal stresses and dislocation-yype defects. Appl Phys Lett 2000;77:1695–7.

[67] Misirlioglu IB, Vasiliev AL, Aindow M, Alpay SP, Ramesh R. Threading dislocation generation in epitaxial (Ba, Sr)TiO_3 films grown on (001) $LaAlO_3$ by pulsed laser deposition. Appl Phys Lett 2004;84:1742–4.

[68] Chu MW, Szafraniak I, Scholz R, Harnagea C, Hesse D, Alexe M, et al. Impact of misfit dislocations on the polarization instability of epitaxial nanostructured ferroelectric perovskites. Nature Mater 2004;3:87–90.

[69] Alpay SP, Misirlioglu IB, Nagarajan V, Ramesh R. Can interface dislocations degrade ferroelectric properties? Appl Phys Lett 2004;85:2044–6.

[70] Nagarajan V, Jia CL, Kohlstedt H, Waser R, Misirlioglu IB, Alpay SP, et al. Misfit dislocations in nanoscale ferroelectric heterostructures. Appl Phys Lett 2005;86:192910.

[71] Fennie CJ, Rabe KM. Magnetic and electric phase control in epitaxial $EuTiO_3$ from first principles. Phys Rev Lett 2006;97:267602.

[72] Rivera JP, Schmid H. Electrical and optical measurements on nickel iodine boracite. Ferroelectrics 1981;36:447–50.

[73] von Wartburg W. The magnetic structure of magnetoelectric nickel-iodine boracite $Ni_3B_7O_{13}I$. Phys, Status Solidi A 1974;21:557–68.

[74] Lee JH, Rabe KM. Epitaxial-strain-induced multiferroicity in $SrMnO_3$ from first principles. Phys Rev Lett 2010;104:207204.

[75] Bousquet E, Spaldin NA, Ghosez P. Strain-induced ferroelectricity in simple rocksalt binary oxides. Phys Rev Lett 2010;104:037601.

[76] Lempicki A, Randles MH, Wisniewski D, Balcerzyk M, Brecher C, Wojtowicz AJ. $LuAlO_3$:Ce and other aluminate scintillators. IEEE Trans Nucl Sci 1995;42:280–5.

[77] Petrosyan AG, Shirinyan GO, Pedrini C, Durjardin C, Ovanesyan KL, Manucharyan RG, et al. Bridgman growth and characterization of $LuAlO_3$—Ce^{3+} scintillator crystals. Cryst Res Technol 1998;33:241–8.

[78] Asano H, Kubo S, Michikami O, Satoh M, Konaka T. Epitaxial growth of $EuBa_2Cu_3O_{7-y}$ films on $YAlO_3$ single crystals. Jpn J Appl Phys Part 2 1990;298:L1452–4.

[79] Brown R, Pendrick V, Kalokitis D, Chai BHT. Low-loss substrate for microwave application of high-temperature superconductor films. Appl Phys Lett 1990;57(13):1351–3.

[80] Miyazawa Y, Toshima H, Morita S. The growth of $NdAlO_3$ single crystals by Czochralski method. J Cryst Growth 1993;128:668–71.

[81] Berkstresser GW, Valentino AJ, Brandle CD. Growth of single crystals of lanthanum aluminate. J Cryst Growth 1991;109(1–4):467–71.

[82] Berkstresser GW, Valentino AJ, Brandle CD. Congruent composition for growth of lanthanum aluminate. J Cryst Growth 1993;128(1–4):684–8.

[83] Hontsu S, Ishii J, Kawai T, Kawai S. $LaSrGaO_4$ substrate gives oriented crystalline $YBa_2Cu_3O_{7-y}$ films. Appl Phys Lett 1991;59(22):2886–8.

[84] Mateika D, Kohler H, Laudan H, Volkel E. Mixed-perovskite substrates for high-T_c superconductors. J Cryst Growth 1991;109(1-4):447–56.

[85] Simon RW, Platt CE, Lee AE, Lee GS, Daly KP, Wire MS, et al. Low-loss substrate for epitaxial growth of high-temperature superconductor thin films. Appl Phys Lett 1988;53(26):2677–9.

[86] Berkstresser GW, Valentino AJ, Brandle CD. Growth of single crystals of rare earth gallates. J Cryst Growth 1991;109(1–4):457–66.

[87] Chakoumakos BC, Schlom DG, Urbanik M, Luine J. Thermal expansion of $LaAlO_3$ and (La, Sr)(Al, Ta)O_3 substrate materials for superconducting thin-film device applications. J Appl Phys 1998;83(4):1979–82.

[88] Sandstrom RL, Giess EA, Gallagher WJ, Segmüller A, Cooper EI, Chisholm MF, et al. Lanthanum gallate substrates for epitaxial high-temperature superconducting thin films. Appl Phys Lett 1988;53(19):1874–6.

[89] Merker L. Method of prepration of monocrystalline strontium titanate composition of high refractive index. US Patent No. 2684,910; 27 July 1954.

[90] Bednorz JG, Scheel HJ. Flame-fusion growth of $SrTiO_3$. J Cryst Growth 1977;41(1):5–12.

[91] Nabokin PI, Souptel D, Balbashov AM. Floating zone growth of high-quality $SrTiO_3$ single crystals. J Cryst Growth 2003;250(3–4):397–404.

[92] Scheel HJ, Bednorz JG, Dill P. Crystal growth of strontium titanate $SrTiO_3$. Ferroelectrics 1976;13(1–4):507–9.

[93] Uecker R, Wilke H, Schlom DG, Velickov B, Reiche P, Polity A, et al. Spiral formation during Czochralski growth of rare-earth scandates. J Cryst Growth 2006;295:84–91.

[94] Uecker R, Velickov B, Klimm D, Bertram R, Bernhagen M, Rabe M, et al. Properties of rare-earth scandate single crystals (Re = Nd—Dy). J Cryst Growth 2008;310:2649–58.

[95] Feenstra R, Boatner LA, Budai JD, Christen DK, Galloway MD, Poker DB. Epitaxial superconducting thin films of $YBa_2Cu_3O_{7-x}$ on $KTaO_3$ single crystals. Appl Phys Lett 1989;54:1063–5.

[96] Coh S, Heeg T, Haeni JH, Biegalski MD, Lettieri J, Edge LF, et al. Si-compatible candidates for high-*k* dielectrics with the *Pbnm* perovskite structure. Phys Rev B 2010;82:064101.

[97] Ihlefeld JF, Tian W, Liu ZK, Doolittle WA, Bernhagen M, Reiche P, et al. Adsorption-controlled growth of $BiFeO_3$ by MBE and integration with wide band gap semiconductors. IEEE Trans Ultras Ferroelectr Freq Control 2009;56:1528–33.

[98] Lee JH, Ke X, Misra R, Ihlefeld JF, Xu XS, Mei ZG, et al. Adsorption-controlled growth of $BiMnO_3$ films by molecular-beam epitaxy. Appl Phys Lett 2010;96:262905.

[99] Kawasaki M, Takahashi K, Maeda T, Tsuchiya R, Shinohara M, Ishiyama O, et al. Atomic control of the $SrTiO_3$ crystal surface. Science 1994:1540–2.

[100] Koster G, Kropman BL, Rijnders GJHM, Blank DHA, Rogalla H. Quasi-Ideal strontium titanate crystal surfaces through formation of strontium hydroxide. Appl Phys Lett 1998;73:2920–2.

[101] Schrott AG, Misewich JA, Copel M, Abraham DW, Zhang Y. *A*-site surface termination in strontium titanate single crystals. Appl Phys Lett 2001;79:1786–8.

[102] Biswas A, Rossen PB, Yang CH, Siemons W, Jung MH, Yang IK, et al. Universal Ti-rich termination of atomically flat $SrTiO_3$ (001), (110), and (111) surfaces. Appl Phys Lett 2011;98:051904.

[103] Chang J, Park YS, Kim SK. Atomically flat single-terminated $SrTiO_3$ (111) surface. Appl Phys Lett 2008;92:152910.

[104] Blok JL, Wan X, Koster G, Blank DHA, Rijnders G. Epitaxial oxide growth on polar (111) surfaces. Appl Phys Lett 2011;99:151917.

[105] Ohnishi T, Takahashi K, Nakamura M, Kawasaki M, Yoshimoto M, Koinuma H. *A*-site Layer terminated perovskite substrate: $NdGaO_3$. Appl Phys Lett 1999;74:2531–3.

[106] Ngai JH, Schwendemann TC, Walker AE, Segal Y, Walker FJ, Altman EI, et al. Achieving A-Site termination on $La_{0.18}Sr_{0.82}Al_{0.59}Ta_{0.41}O_3$ substrates. Adv Mater 2010;22:2945–8.

[107] Kleibeuker JE, Koster G, Siemons W, Dubbink D, Kuiper B, Blok JL, et al. Atomically defined rare-earth scandate crystal surfaces. Adv Mater 2010;20:3490–6.

[108] Bae HJ, Sigman J, Norton DP, Boatner LA. Surface treatment for forming unit-cell steps on the (001) $KTaO_3$ substrate surface. Appl Surf Sci 2005;241:271–8.

[109] Cho AY, Arthur JR. Molecular beam epitaxy. Prog Solid State Chem 1975;10:157–91.

[110] Farrow RFC, editor. Molecular beam epitaxy: applications to key materials. Park Ridge: Noyes; 1995.

[111] Herman MA, Sitter H. Molecular beam epitaxy: fundamentals and current status. second ed. Berlin: Springer-Verlag; 1996.

[112] Yoshida S. Reactive molecular beam epitaxy. In: Schuele DE, Hoffman RW, editors. Critical reviews™ in solid state and materials sciences, vol. 11. Boca Raton: CRC Press; 1984. p. 287–316.

[113] Iijima K, Terashima T, Yamamoto K, Hirata K, Bando Y. Preparation of ferroelectric $BaTiO_3$ thin films by activated reactive evaporation. Appl Phys Lett 1990;56:527–9.

[114] Endo K, Saya S, Misawa S, Yoshida S. Preparation of yttrium barium copper oxide superconducting films by metalorganic molecular beam epitaxy. Thin Solid Films 1991;296:143–5.

[115] King LLH, Hsieh KY, Lichtenwalner DJ, Kingon AI. In situ deposition of superconducting $YBa_2Cu_3O_{7-x}$ and $DyBa_2Cu_3O_{7-x}$ thin films by organometallic molecular-beam epitaxy. Appl Phys Lett 1991;59:3045–7.

[116] Jalan B, Engel-Herbert R, Wright NJ, Stemmer S. Growth of high-quality SrTiO3 films using a hybrid molecular beam epitaxy approach. J Vac Sci Technol A 2009;27:461–4.

[117] Mori H, Ishiwara H. Epitaxial growth of $SrTiO_3$ films on Si(100) substrates using a focused electron beam evaporation method. Jpn J Appl Phys 1991;30:L1415–7.

[118] McKee RA, Walker FJ, Chisholm MF. Crystalline oxides on silicon: the first five monolayers. Phys Rev Lett 1998;81:3014–7.

[119] Eisenbeiser K, Finder JM, Yu Z, Ramdani J, Curless JA, Hallmark JA, et al. Field effect transistors with $SrTiO_3$ gate dielectric on Si. Appl Phys Lett 2000;76:1324–6.

[120] Yu Z, Ramdani J, Curless JA, Overgaard CD, Finder JM, Droopad R, et al. Epitaxial oxide thin films on Si(001). J Vac Sci Technol B 2000;18:2139–45.

[121] McKee RA, Walker FJ, Chisholm MF. Physical structure and inversion charge at a semiconductor interface with a crystalline oxide. Science 2001;293:468–71.

[122] Lettieri J. Critical issues of complex, epitaxial oxide growth and integration with silicon by molecular beam epitaxy. Ph.D. thesis, Pennsylvania State University; 2002. <http://etda.libraries.psu.edu/theses/approved/WorldWideIndex/ETD-202/index.html>.

[123] Li H, Hu X, Wei Y, Yu Z, Zhang X, Droopad R, et al. Two-dimensional growth of high-quality strontium titanate thin films on Si. J Appl Phys 2003;93:4521–5.

[124] Walker FJ, McKee RA. High-k crystalline gate dielectrics: a research perspective. In: Huff HR, Gilmer DC, editors. High dielectric constant materials: VLSI MOSFET applications. Berlin: Springer; 2005. p. 607–37.

[125] Fitting Kourkoutis L, Hellberg CS, Vaithyanathan V, Li H, Parker MK, Andersen KE, et al. Imaging the phase separation in atomically thin buried $SrTiO_3$ layers by electron channeling. Phys Rev Lett 2008;100:036101.

[126] Reiner JW, Kolpak AM, Segal Y, Garrity KF, Ismail-Beigi S, Ahn CH, et al. Crystalline oxides on silicon. Adv Mater 2010;22:2919–38.

[127] Tsukazaki A, Akasaka S, Nakahara K, Ohno Y, Ohno H, Maryenko D, et al. Observation of the fractional quantum hall effect in an oxide. Nature Mater 2010;9:889–93.

[128] Falson J, Maryenko D, Kozuka Y, Tsukazaki A, Kawasaki M. Magnesium doping controlled density and mobility of two-dimensional electron gas in $Mg_xZn_{1-x}O$/ZnO heterostructures. Appl Phys Exp 2011;4:091101.

[129] Tsukazaki A, Ohtomo A, Kita T, Ohno Y, Ohno H, Kawasaki M. Quantum hall effect in polar oxide heterostructures. Science 2007;315:1388–91.

[130] Eisenstein JP, Cooper KB, Pfeiffer LN, West KW. Insulating and fractional quantum hall states in the first excited landau level. Phys Rev Lett 2002;88:076801.

[131] Pfeiffer L, West KW. The role of MBE in recent quantum hall effect physics discoveries. Physica E 2003;20:57–64.
[132] Umansky V, Heiblum M, Levinson Y, Smet J, Nübler J, Dolev M. MBE growth of ultra-low disorder 2DEG with mobility exceeding 35106 ×106cm2/V s. J Cryst Growth 2009;311:1658–61.
[133] Biegalski MD, Jia Y, Schlom DG, Trolier-McKinstry S, Streiffer SK, Sherman V, et al. Relaxor ferroelectricity in strained epitaxial $SrTiO_3$ thin films on $DyScO_3$ substrates. Appl Phys Lett 2006;88:192907.
[134] Schlom DG, Chen LQ, Eom CB, Rabe KM, Streiffer SK, Triscone JM. Strain tuning of ferroelectric thin films. Annu Rev Mater Res 2007;37:589–626.
[135] Biegalski MD, Fong DD, Eastman JA, Fuoss PH, Streiffer SK, Heeg T, et al. Critical thickness of high structural quality $SrTiO_3$ films grown on orthorhombic (101) $DyScO_3$. J Appl Phys 2008;104:114109.
[136] Schlom DG, Chen LQ, Pan XQ, Schmehl A, Zurbuchen MA. A thin film approach to engineering functionality into oxides. J Am Ceram Soc 2008;91:2429–54.
[137] Sakamoto T, Funabashi H, Ohta K, Nakagawa T, Kawai NJ, Kojima T, et al. Well defined superlattice structures made by phase-locked epitaxy using RHEED intensity oscillations. Superlatt Microstruct 1985;1:347–52.
[138] Gossard AC, Petroff PM, Weigmann W, Dingle R, Savage A. Epitaxial structures with alternate-atomic-layer composition modulation. Appl Phys Lett 1976;29:323–5.
[139] Cho AY. Molecular beam epitaxy from research to manufacturing. MRS Bull 1995;20:21–8.
[140] Schlom DG, Eckstein JN, Bozovic I, Chen ZJ, Marshall AF, von Dessonneck KE, et al. Molecular beam epitaxy—a path to novel high Tc superconductors? In: Growth of semiconductor structures and high-tc thin films on semiconductors, SPIE, vol. 1285, 1990; SPIE, Bellingham. p. 234–47.
[141] Eckstein J, Bozovic I. High-temperature superconducting multilayers and heterostructures grown by atomic layer-by-layer molecular beam epitaxy. Annu Rev Mater Sci 1995;25:679–709.
[142] Schlom DG, Harris Jr JS. MBE growth of high T_c superconductors. In: Farrow RFC, editor. Molecular beam epitaxy: applications to key materials. Park Ridge: Noyes; 1995. p. 505–622.
[143] Bozovic I, Eckstein JN. Superconducting superlattices. In: Ginsberg DM, editor. Physical properties of high temperature superconductors V. Singapore: World Scientific; 1996. p. 99–207.
[144] Jiang JC, Pan XQ, Tian W, Theis CD, Schlom DG. Abrupt $PbTiO_3/SrTiO_3$ superlattices grown by reactive molecular beam epitaxy. Appl Phys Lett 1999;74:2851–3.
[145] Warusawithana MR, Colla EV, Eckstein JN, Weissman MB. Artificial dielectric superlattices with broken inversion symmetry. Phys Rev Lett 2003;90:036802.
[146] Bozovic I, Logvenov G, Verhoeven MAJ, Caputo P, Goldobin E, Geballe TH. No mixing of superconductivity and antiferromagnetism in a high-temperature superconductor. Nature 2003;422:873–5.
[147] Ahn CH, Rabe KM, Triscone JM. Ferroelectricity at the nanoscale: local polarization in oxide thin films and heterostructures. Science 2004;303:488–91.
[148] Tenne DA, Bruchhausen A, Lanzillotti-Kimura ND, Fainstein A, Katiyar RS, Cantarero A, et al. Probing nanoscale ferroelectricity by ultraviolet raman spectroscopy. Science 2006;313:1614–6.
[149] Haeni JH, Theis CD, Schlom DG, Tian W, Pan XQ, Chang H, et al. Epitaxial growth of the first five members of the $Sr_{n+1}Ti_nO_{3n+1}$ Ruddlesden-Popper homologous series. Appl Phys Lett 2001;78:3292–4.
[150] Tian W, Haeni JH, Schlom DG, Hutchinson E, Sheu BL, Rosario MM, et al. Epitaxial growth and magnetic properties of the first five members of the layered $Sr_{n+1}Ru_nO_{3n+1}$ oxide series. Appl Phys Lett 2007;90:022507.
[151] Heeg T, Roeckerath M, Schubert J, Zander W, Buchal C, Chen HY, et al. Epitaxially stabilized growth of orthorhombic $LuScO_3$ thin films. Appl Phys Lett 2007;90:192901.
[152] Kitabatake M, Fons P, Greene JE. Molecular dynamics simulations of low-energy particle bombardment effects during vapor-phase crystal growth: 10 eV Si atoms incident on Si(001)2 × 1 surfaces. J Vac Sci Technol A 1990;8:3726–35.
[153] Kitabatake M, Greene JE. Molecular dynamics and quasidynamics simulations of low-energy particle bombardment effects during vapor-phase crystal growth: production and annihilation of defects due to 50 eV Si incident on (2 × 1)-terminated Si(001). J Appl Phys 1993;73:3183–94.
[154] Tarsa EJ, Hachfeld EA, Quinlan FT, Speck JS, Eddy M. Growth-related stress and surface morphology in homoepitaxial $SrTiO_3$ films. Appl Phys Lett 1996;68:490–2.
[155] Maria JP, Trolier-McKinstry S, Schlom DG, Hawley ME, Brown GW. The influence of energetic bombardment on the structure and properties of epitaxial $SrRuO_3$ thin films grown by pulsed laser deposition. J Appl Phys 1998;83:4373–9.
[156] Ohnishi T, Lippmaa M, Yamamoto T, Meguro S, Koinuma H. Improved stoichiometry and misfit control in perovskite thin film formation at a critical fluence by pulsed laser deposition. Appl Phys Lett 2005;87:2419191.
[157] Ohnishi T, Shibuya K, Yamamoto T, Lippmaa M. Defects and transport in complex oxide thin films. J Appl Phys 2008;103:103703.
[158] Ihlefeld JF, Podraza NJ, Liu ZK, Rai RC, Xu X, Heeg T, et al. Optical band gap of $BiFeO_3$ grown by molecular-beam epitaxy. Appl Phys Lett 2008;92:142908.
[159] Xu XS, Ihlefeld JF, Lee JH, Ezekoye OK, Vlahos E, Ramesh R, et al. Tunable band gap in $Bi(Fe_{1-x}Mn_x)O_3$ films. Appl Phys Lett 2010;96:192901.
[160] Chrisey DB, Hubler GK. Pulsed laser deposition of thin films. New York: John Wiley & Sons, Inc.; 1994.
[161] Eason R. Pulsed laser deposition of thin films: applications-led growth of functional materials. Hoboken, NJ: John Wiley & Sons; 2007.
[162] Christen HM, Eres G. Recent advances in pulsed-laser deposition of complex oxides. J Phys Condens Matter 2008;20:264005.
[163] Kim DH, Lee HN, Biegalski MD, Christen HM. Large ferroelectric polarization in antiferromagnetic $BiFe_{0.5}Cr_{0.5}O_3$ epitaxial films. Appl Phys Lett 2007;91:042906.
[164] Rijnders G, Blank DHA. In: Auciello O, Ramesh R, editors. Thin films and heterostructures of oxide electronics. New York: Springer; 2005.
[165] Huijben M, Martin LW, Chu YH, Holcomb MB, Yu P, Rijnders G, et al. Critical thickness and orbital ordering in ultrathin $La_{0.7}Sr_{0.3}MnO_3$ films. Phys Rev B 2008;78:094413.
[166] Koinuma H, Kawasaki M, Ohashi S, Lippmaa M, Nakagawa N, Iwasaki M, et al. Nucleation and growth control in pulsed laser epitaxy of oxide thin films. Proc SPIE 1998;3481:153–60.
[167] Ohashi S, Lippmaa M, Nakagawa N, Nasagawa H, Koinuma H, Kawasaki M. Compact laser molecular beam epitaxy system using laser heating of substrate for oxide film growth. Rev Sci Instrum 1999;70:178–83.
[168] Chen P, Xu SY, Lin J, Ong CK, Cui DF. Angle-resolved X-ray photoelectron spectroscopy of topmost surface for $LaNiO_3$ thin film grown on $SrTiO_3$ substrate by laser molecular beam epitaxy. Appl Surf Sci 1999;137:98–102.
[169] Yang GZ, Lu HB, Chen F, Zhao T, Chen ZH. Laser molecular beam epitaxy and characterization of perovskite oxide thin films. J Cryst Growth 2001;227–228:929–35.
[170] Hasegawa S, Ino S, Yamamoto Y, Daimon H. Chemical analysis of surfaces by total-reflection-angle x-ray spectroscopy in RHEED experiments (RHEED-TRAXS). Jpn J Appl Phys 1985;24:L387–90.
[171] Krauss AR, Rangaswamy M, Lin Y, Gruen DM, Schultz JA, Schmidt HK, et al. In: Auciello O, Engemann J, editors. Multicomponent and multilayered thin films for advanced microtechnologies, techniques, fundamentals, and devices. The Netherlands: Kluwer; 1993.
[172] Krauss AR, Lin Y, Auciello O, Lamich GJ, Gruen DM, Schultz JA, et al. Pulsed ion beam surface analysis as a means of in situ real-time analysis of thin films during growth. J Vac Sci Technol A 1994;12:1943–51.
[173] Lin Y, Krauss AR, Chang RPH, Auciello O, Gruen DM, Schultz JA. Atmosphere influence on the in-situ ion beam analysis of thin film growth. Thin Solid Films 1995;253:247–53.
[174] Hammond MS, Schultz JA, Krauss AR. Surface analysis at low to ultrahigh vacuum by ion scattering and direct recoil spectroscopy. J Vac Sci Technol A 1995;13:1136–44.
[175] Yu P, Luo W, Yi D, Zhang J, Rossell M, Yang CH, et al. Interface control of bulk ferroelectric polarization. Proc Nat Acad Sci, accepted for publication.
[176] http://www.utwente.nl/tnw/ims/pictures/Research/interface/research_broekmaat.doc/.
[177] Horiba K, Ohguchi H, Kumigashira H, Oshima M, Ono K, Nakagawa N, et al. A high-resolution synchrotron-radiation angle-resolved photoemission spectrometer with *in situ* oxide thin film growth capability. Rev Sci Instrum 2003;74:3406–12.
[178] Eres G, Tischler JZ, Yoon M, Larson BC, Rouleau CM, Lowndes DH, et al. Time-resolved study of $SrTiO_3$ homoepitaxial pulsed-laser deposition using surface x-ray diffraction. Appl Phys Lett 2002;80:3379–81.
[179] Eres G, Tischler JZ, Rouleau CM, Larson BC, Christen HM, Zschack P. Real-time studies of epitaxial film growth using surface x-ray diffraction (SXRD). In: Koster G, Rijnders G, editors. *In situ* characterization of thin film growth. Philadelphia, PA: Woodhead Publishing; 2011.
[180] Vonk V, Konings S, Barthe L, Gorges B, Graafsma H. Pulsed laser deposition chamber for *in situ* X-ray diffraction. J Synchrotron Rad 2005;12:833–4.
[181] Dale D, Suzuki Y, Brock JD. *In situ* x-ray reflectivity studies of dynamics and morphology during heteroepitaxial complex oxide thin film growth. J Phys Condens Matter 2008;20:264008.
[182] Wasa K, Kitabatake M, Abachi H. Thin film materials technology – sputtering of compound materials. Norwich, NY: William Andrew Publishing; 2004.
[183] Fujimura N, Ishida T, Yoshimura T, Ito T. Epitaxially grown $YMnO_3$ film: new candidate for nonvolatile memory devices. Appl Phys Lett 1996;69:1011–3.
[184] Das RR, Kim DM, Baek SH, Eom CB, Zavaliche F, Yang SY, et al. Synthesis and ferroelectric properties of epitaxial $BiFeO_3$ thin films grown by sputtering. Appl Phys Lett 2006;88:242904.
[185] Leskelä A, Mölsä H, Niinistö L. Chemical vapour deposition of high-T_C superconducting thin films. Supercond Sci Technol 1993;6:627–56.
[186] Yang SY, Zavaliche F, Mohaddes-Ardabili L, Vaithyanathan V, Schlom DG, Lee YJ, et al. Metalorganic chemical vapor deposition of lead-free ferroelectric $BiFeO_3$ films for memory applications. Appl Phys Lett 2005;87:102903.
[187] Singh MK, Yang Y, Takoudis CG. Synthesis of multifunctional multiferroic materials from metalorganics. Coordination Chem Rev 2009;253:2920–34.
[188] Wantanabe T, Hoffman-Eifert S, Hwang CS, Waser R. Growth behavior of atomic-layer-deposited Pb(Zr, Ti)Ox thin films on planar substrate and three-dimensional hole structures. J Electrochem Soc 2008;155:D715–22.
[189] Nilsen O, Rauwel E, Fjellvåg H, Kjekshus A. Growth of $La_{1-x}Ca_xMnO_3$ thin films by atomic layer deposition. J Chem Mater 2007;17:1466–75.
[190] Gandrud KB. Master thesis, Thin films of multiferroic $BiCoO_3$ by ALD. University of Olso; 2009. <http://www.duo.uio.no/sok/work.html?WORKID=95492&lang=en>.
[191] Choi JH, Pham CD, Chang JP. Engineered multiferroic PZT-CFO and BFO-CFO thin films for large magnetoelectric coefficient by atomic layer deposition.

Presented at 2011 AIChE annual meeting, Minneapolis, MN; Wednesday October 19, 2011.
[192] Uusi-Esko K, Karppinen M. Extensive series of hexagonal and orthorhombic $RMnO_3$ (R = Y, La, Sm, Tb, Yb, Lu) thin films by atomic layer deposition. Chem Mater 2011;23:1835–40.
[193] Kimura T, Lawes G, Goto T, Tokura Y, Ramirez AP. Magnetoelectric phase diagrams of orthorhombic $RMnO_3$ (R = Gd, Tb, and Dy). Phys Rev B 2005;71:224425.
[194] Lottermoser T, Lonkai T, Amann U, Hohlwein D, Ihringer J, Fiebig M. Magnetic phase control by an electric field. Nature 2004;430:541–4.
[195] Yakel HL, Koehler WD, Bertaut EF, Forrat F. On the crystal structure of the manganese (III) trioxides of the heavy lanthanides and yttrium. Acta Crystalogr 1963;16:957–62.
[196] Shukla DK, Kumar R, Sharma SK, Thakur P, Choudhary RJ, Mollah S, et al. Thin film growth of multiferroic $BiMn_2O_5$ using pulsed laser ablation and its characterization. J Phys D 2009;42:125304.
[197] Sai N, Fennie CJ, Demkov AA. Absence of critical thickness in an ultrathin improper ferroelectric film. Phys Rev Lett 2009;102:107601.
[198] Skumryev V, Laukhin V, Fina I, Martí X, Sánchez F, Gosodinov M, et al. Magnetization reversal by electric-field decoupling of magnetic and ferroelectric domain walls in multiferroic-based heterostructures. Phys Rev Lett 2011;106:057206.
[199] Gélardt I, Jehanathan N, Roussel H, Gariglio S, Lebedev OI, Van Tendeloo G, et al. Off-stoichiometry effects on the crystalline and defect structure of hexangonal manganite $REMnO_3$ films (RE = Y, Er, Dy). Chem Mater 2011;23:1232–8.
[200] Sugawara F, Iida S. New magnetic perovskites $BiMnO_3$ and $BiCrO_3$. J Phys Soc Jpn 1965;20:1529.
[201] Faqir H, Chiba H, Kikuchi M, Syono Y, Mansori M, Satre P, et al. High-temperature XRD and DTA studies of $BiMnO_3$ perovskite. J Solid State Chem 1999;142:113–9.
[202] Atou T, Chiba H, Ohoyama K, Yamaguchi Y, Syono Y. Structure determination of ferromagnetic perovskite $BiMnO_3$. J Solid State Chem 1999;145:639–42.
[203] Ohshima E, Saya Y, Nantoh M, Kawai M. Synthesis and magnetic property of the perovskite $Bi_{1-x}Sr_xMnO_3$ thin film. Solid State Commun 2000;116:73–6.
[204] Atou T, Chiba H, Ohoyama K, Yamaguichi Y, Syono Y. Structure determination of ferromagnetic perovskite $BiMnO_3$. J Solid State Chem 1999;145:639–42.
[205] Son JY, Kim BG, Kim CH, Cho YH. Writing polarization bits on the multiferroic $BiMnO_3$ thin film using Kelvin probe force mircroscopy. Appl Phys Lett 2004;84:4971–3.
[206] Gajek M, Bibes M, Fusil S, Bouzehouane K, Fontcuberta J, Barthélémy A, et al. Tunnel junctions with multiferroic barriers. Nature Mater 2007;6:296–302.
[207] Yang CH, Lee SH, Koo TY, Jeong YH. Dynamically enhanced magnetodielectric effect and magnetic-field-controlled electric relaxations in La-doped $BiMnO_3$. Phys Rev B 2007;75:140104.
[208] Baettig P, Seshadri R, Spaldin NA. Anti-polarity in ideal $BiMnO_3$. J Am Chem Soc 2007;129:9854–5.
[209] Belik AA, Kolodiazhnyi T, Kosuda K, Takayama-Muromachi E. Synthesis and properties of oxygen non-stoichiometric $BiMnO_3$. J Mater Chem 2009;19:1593–600.
[210] Hill NA, Battig PA, Daul C. First principles search for multiferroism in $BiCrO_3$. J Phys Chem B 2002;106:3383–8.
[211] Murakami M, Fujino S, Lim SH, Long CJ, Salamanca-Riba LG, Wuttig M, et al. Fabrication of multiferroic $BiCrO_3$ thin films. Appl Phys Lett 2006;88:152902.
[212] Kim DH, Lee HN, Varela M, Christen HM. Antiferroelectricity in multiferroic $BiCrO_3$ epitaxial films. Appl Phys Lett 2006;89:162904.
[213] Belik AA, Iikubo S, Kodama K, Igawa N, Shamota S, Niitaka S, et al. Neutron powder diffraction study on the crystal and magnetic structures of $BiCrO_3$. Chem Mater 2006;18:798–803.
[214] Urantani Y, Shishidou T, Ishii F, Oguchi T. First-principles predictions of giant electric polarization. Jpn J Appl Phys 2005;44:7130–3.
[215] Yasui S, Nishida K, Naganuma H, Okamura S, Iijima T, Funakubo H. Crystal structure analysis of epitaxial $BiFeO_3$-$BiCoO_3$ solid solution films grown by metalorganic chemical vapor deposition. Jpn J Appl Phys 2007;46:6948–51.
[216] Nakamura Y, Kawai M, Azuma M, Kubota M, Shimada M, Aiba T, et al. Enhanced piezoelectric constant of (1-x)$BiFeO_3$-x$BiCoO_3$ thin films grown on $LaAlO_3$ substrate. Jpn J Appl Phys 2011;50:031505.
[217] Martin LW, Zhan Q, Suzuki Y, Ramesh R, Chi M, Browning N, et al. Growth and structure of $PbVO_3$ thin films. Appl Phys Lett 2007;90:062903.
[218] Kumar A, Martin LW, Denev S, Kortright JB, Suzuki Y, Ramesh R, et al. Polar and magnetic properties of $PbVO_3$ thin films. Phys Rev B 2007;75:060101. R.
[219] Sakai M, Msauno A, Kan D, Hashisaka M, Takata K, Azume M, et al. Multiferroic thin film of Bi_2NiMnO_6 with ordered double-perovskite structure. Appl Phys Lett 2007;90:072903.
[220] McGuire TR, Shafer MW, Joenk RJ, Alperin HA, Pickart SJ. Magnetic structure of $EuTiO_3$. J Appl Phys 1966;37:981–2.
[221] Chien CL, DeBenedetti S, Barros FDS. Magnetic properties of $EuTiO_3$, Eu_2TiO_4, and $Eu_3Ti_2O_7$. Phys Rev B 1974;10:3913–22.
[222] Katsufuji T, Takagi H. Coupling between magnetism and dielectric properties in quantum paraelectric $EuTiO_3$. Phys Rev B 2001;64:054415.
[223] Wang HH, Fleet A, Brock JD, Dale D, Suzuki Y. Nearly strain-free heteroepitaxial system for fundamental studies of pulsed laser deposition: $EuTiO_3$ on $SrTiO_3$. J Appl Phys 2004;96:5324–8.
[224] Kugimiya K, Fujita K, Tanaka K, Hirao K. Preparation and magnetic properties of oxygen deficient $EuTiO_{3-\delta}$ thin films. J Magn Magn Mater 2007;310: 2268–70.
[225] Chae SC, Chang YJ, Kim DW, Lee BW, Choi I, Jung CU. Magnetic properties of insulating $RTiO_3$ thin films. J Electroceram 2009;22:216–20.
[226] Fujita K, Wakasugi N, Murai S, Zong Y, Tanaka K. High-quality antiferromagnetic $EuTiO_3$ epitaxial thin films on $SrTiO_3$ prepared by pulsed laser deposition and postannealing. Appl Phys Lett 2009;94:062512.
[227] Schafer MW. Preparation and crystal chemistry of divalent europium compounds. J Appl Phys 1965;36:1145–52.
[228] McCarthy GJ, White WB, Roy R. The system Eu-Ti-O: phase relations in a portion of the 1400°C isotherm. J Inorg Nucl Chem 1969;31:329–40.
[229] Kim YS, Kim DJ, Kim TH, Noh TW, Choi JS, Park BH, et al. Observation of room-temperature ferroelectricity in tetragonal strontium titanate thin films on $SrTiO_3$ (001) substrates. Appl Phys Lett 2007;91:042908.
[230] Müller KA, Burkard H. $SrTiO_3$: an intrinsic quantum paraelectric below 4K. Phys Rev B 1979;19:3593–602.
[231] Kestigian M, Dickinson JG, Ward R. Ion-deficient phases in titanium and vanadium compounds of the perovskite type. J Am Chem Soc 1957;79:5598–601.
[232] Tenne DA, Gonenli IE, Soukiassian A, Schlom DG, Nakhmanson SM, Rabe KM, et al. Raman study of oxygen reduced and re-oxidized strontium titanate. Phys Rev B 2007;76:024303.
[233] Brooks CM. Fitting Kourkoutis L, Heeg T, Schubert J, Muller DA, Schlom DG. Growth of homoepitaxial $SrTiO_3$ thin films by molecular-beam epitaxy. Appl Phys Lett 2009;94:162905.
[234] Breckenfeld E, Wilson R, Karthik J, Damodaran AR, Cahill DG, Martin LW. Effect of growth induced (non)stoichiometry on the structure, dielectric response, and thermal conductivity of $SrTiO_3$ thin films. Chem Mater 2012;24:331–7.
[235] Lee JH, Ke X, Podraza NJ, Fitting Kourkoutis L, Heeg T, Roeckerath M, et al. Optical band gap and magnetic properties of unstrained $EuTiO_3$ films. Appl Phys Lett 2009;94:212509.
[236] Royen P, Swars K. Das system wismutoxyd-eisenoxyd im bereich von 0 bis 55 mol% eisenoxyd. Angew Chem 1957;24:779.
[237] Zavaliche F, Yang SY, Zhao T, Chu YH, Cruz MP, Eom CB, et al. Multiferroic $BiFeO_3$ films: domain structure and polarization dynamics. Phase Transit 2006;79:991–1017.
[238] Lebeugle D, Colson D, Forget A, Viret M, Bonville P, Marucco JF, et al. Room-temperature coexistence of large electric polarization and magnetic order in $BiFeO_3$ single crystals. Phys Rev B 2007;76:024116.
[239] Fischer P, Polomska M, Sosnowska I, Szymanski M. Temperature dependence of the crystal and magnetic structures of $BiFeO_3$. J Phys C 1980;13:1931–40.
[240] Sosnowska I, Peterlin-Neumaier T, Steichele E. Spiral magnetic ordering in bismuth ferrite. J Phys C 1982;15:4835–46.
[241] Dzyaloshinskii IE. Thermodynamic theory of weak ferromagnetism in antiferromagnetic substances. Sov Phys JETP 1957;5:1259–72.
[242] Moriya T. Anisotropic superexchange interaction and weak ferromagnetism. Phys Rev 1960;120:91–8.
[243] Holcomb MB, Martin LW, Scholl A, He Q, Yu P, Yang CH, et al. Probing the evolution of antiferromagnetism in multiferroics. Phys Rev B 2010;81:134406.
[244] Chu YH, Zhan Q, Martin LW, Cruz MP, Yang PL, Pabst GW, et al. Nanoscale domain control in multiferroic $BiFeO_3$ thin films. Adv Mater 2006;18:2307–11.
[245] Pabst GW, Martin LW, Chu YH, Ramesh R. Leakage mechanisms in $BiFeO_3$ thin films. Appl Phys Lett 2007;90:072902.
[246] Chu YH, Cruz MP, Yang CH, Martin LW, Yang PL, Zhang JX, et al. Domain control in multiferroic $BiFeO_3$ through substrate vicinality. Adv Mater 2007;19:2662–6.
[247] Streiffer SK, Parker CB, Romanov AE, Lefevre MJ, Zhao L, Speck JS, et al. Domain patterns in epitaxial rhombohedral ferroelectric films. I. geometry and epxeriments. J Appl Phys 1998;83:2742–53.
[248] Chu YH, He Q, Yang CH, Yu P, Martin LW, Shafer P, et al. Nanoscale control of domain architectures in $BiFeO_3$ thin films. Nano Lett 2009;9:1726–30.
[249] Martin LW, Chu YH, Holcomb MB, Huijben M, Han SJ, Lee D, et al. Nanoscale control of exchange bias with $BiFeO_3$ thin films. Nano Lett 2008;8:2050–5.
[250] Daraktchiev M, Catalan G, Scott JF. Landau theory of ferroelectric domain walls in magnetoelectrics. Ferroelectrics 2008;375:122–31.
[251] Catalan G, Scott JF. Physics and applications of bismuth ferrite. Adv Mater 2009;21:2463–85.
[252] He Q, Yeh CH, Yang JC, Singh-Bhalla G, Liang CW, Chiu PW, et al. Magnetotransport at domain walls in $BiFeO_3$. Phys Rev Lett 2012;108:067203.
[253] Seidel J, Martin LW, He Q, Zhan Q, Chu YH, Rother A, et al. Conduction at domain walls in oxide multiferroics. Nature Mater 2009;8:229–34.
[254] Meyer B, Vanderbilt D. *Ab initio* study of ferroelectric domain walls in $PbTiO_3$. Phys Rev B 2002;65:104111.
[255] Seidel J, Maksymovych P, Batra Y, Katan A, Yang SY, He Q, et al. Domain wall conductivity in La-doped $BiFeO_3$. Phys Rev Lett 2010;105:197603.
[256] Maksymovych P, Seidel J, Chu YH, Wu P, Baddorf AP, Chen LQ, et al. Dynamic conductivity of ferroelectric domain walls in $BiFeO_3$. Nano Lett 2011;11:1906–12.
[257] Guyonnet J, Gaponenko I, Gariglio S, Paruch P. Conduction at domain walls in insulating $Pb(Zr_{0.2}Ti_{0.8})O_3$ thin films. Adv Mater 2011;23:5377–82.
[258] Tsui DC, Stormer HL, Gossard AC. Two-dimensional magnetotransport in extreme quantum limit. Phys Rev Lett 1982;48:1559–62.
[259] Michel C, Moreau JM, Achenbach GD, Gerson R, James WJ. Atomic structures of two rhombohedral ferroelectric phases in the Pb(Zr, Ti)O_3 solid solution series. Solid State Commun 1969;7:865–8.

[260] Moreau JM, Michel C, Gerson R, James WJ. Ferroelectric $BiFeO_3$ X-ray and neutron diffraction study. J Phys Chem Solids 1971;32:1315–20.

[261] Kubel F, Schmid H. Structure of a ferroelectric and ferroelastic monodomain crystal of the perovskite $BiFeO_3$. Acta Cryst 1990;B46:698–702.

[262] Ederer C, Spaldin NA. Effect of epitaxial strain on the spontaneous polarization of thin film ferroelectrics. Phys Rev Lett 2005;95:257601.

[263] Ravindran P, Vidya R, Kjekshus A, Fjellvåg H. Theoretical investigation of magnetoelectric behavior in $BiFeO_3$. Phys Rev B 2006;74:224412.

[264] Ricinschi D, Yun KY, Okuyama M. A mechanism for the 150 μC cm^{-2} polarization of $BiFeO_3$ films based on first-principles calculations and new structural data. J Phys Condens Matter 2006;18:L97–L105.

[265] Dupé B, Infante IC, Geneste G, Janolin PE, Bibes M, Barthélémy A, et al. Competing phases in $BiFeO_3$ thin films under compressive epitaxial strain. Phys Rev B 2010;81:144128.

[266] Mazumdar D, Shelke V, Iliev M, Jesse S, Kumar A, Kalinin SV, et al. Nanoscale switching characteristics of nearly tetragonal $BiFeO_3$ thin films. Nano Lett 2010;10:2555–61.

[267] Kumar A, Denev S, Zeches RJ, Vlahos E, Podraza NJ, Melville A, et al. Probing mixed tetragonal/rhombohedral-like monoclinic phases in strained bismuth ferrite films by optical second harmonic generation. Appl Phys Lett 2010;97:112903.

[268] Damodaran AR, Lee S, Kartik J, MacClaren S, Martin LW. Temperature and thickness evolution and epitaxial breakdown in highly-strained $BiFeO_3$ thin films. Phys Rev B 2012;85:024113.

[269] Damodaran AR, Breckenfeld E, Choquette AR, Martin LW. Stabilization of mixed-phase structures in highly strained $BiFeO_3$ thin films via chemical-alloying. Appl Phys Lett 2012;100:082904.

[270] Zhang JX, Xiang B, He Q, Seidel J, Zeches RJ, Yu P, et al. Large field-induced strains in a lead-free piezoelectric material. Nature Nanotechnol 2011;6: 98–102.

[271] Scott JF. Iso-structural phase transitions in $BiFeO_3$. Adv Mater 2010;22: 2106–7.

[272] Ouyang J, Zhang W, Huang X, Roytburd AL. Thermodynamics of formation of tetragonal and rhombohedral heterophase polydomains in epitaxial ferroelectric thin films. Acta Mater 2011;59:3779–91.

[273] Damodaran AR, Liang CW, He Q, Peng CY, Chang L, Chu YH, et al. Nanoscale structure and mechanism for enhanced electromechanical response of highly strained $BiFeO_3$ thin films. Adv Mater 2011;23:3170–5.

[274] Vasudevan RK, Liu Y, Li J, Liang WI, Kumar A, Jesse S, et al. Nanoscale control of phase variants in strain-engineered $BiFeO_3$. Nano Lett 2011;11:3346–54.

[275] He Q, Chu YH, Heron JT, Yang SY, Liang WI, Kuo CY, et al. Electrically controllable spontaneous magnetism in nanoscale mixed phase multiferroics. Nature Commun 2011;2:225.

[276] Ko KT, Jung MH, He Q, Lee JH, Woo CS, Chu K, et al. Concurrent transition of ferroelectric and magnetic ordering near room temperature. Nature Commun 2011;2:567.

[277] MacDougall GW, Christen HM, Siemons W, Biegalski MD, Zarestky JL, Liang S, et al. Antiferromagnetic transitions. In: "T-like" BiFeO3. arXiv:1107.2975v1.

[278] Kreisel J, Jadhav P, Chaix-Pluchery O, Varela M, Dix N, Sanchez F, et al. A phase transition close to room temperature in $BiFeO_3$ thin films. J Phys Condens Matter 2011;23:342202.

[279] Siemons W, Biegalski MD, Nam JH, Christen HM. Temperature-driven structural phase transition in tetragonal-like $BiFeO_3$. Appl Phys Express 2011;4:095801.

[280] Choi KY, Do SH, Lemmens P, Wulferding D, Woo CS, Lee JH, et al. Anomalous low-energy phonons in nearly tetragonal $BiFeO_3$ thin films. Phys Rev B 2011;84:132408.

[281] Wojdel JC, Íñiguez J. Ab initio indications for giant magnetoelectric effects driven by structural softness. Phys Rev Lett 2010;105:037208.

[282] Kitagawa Y, Hiraoka Y, Honda T, Ishikura T, Nakamura H, Kimura T. Low-field magnetoelectric effect at room temperature. Nature Mater 2010;9: 797–802.

[283] Bossak AA, Graboy IE, Gorbenko OY, Kaul AR, Kartavtseva MS, Svetchnikov VL, et al. XRD and HREM studies of epitaxially stabilized hexagonal orthoferrites $RFeO_3$ (R = Eu-Lu). Chem Mater 2004;16:1751–5.

[284] Akbashev AR, Semisalova AS, Perov NS, Kaul AR. Weak ferromagnetism in hexagonal orthoferrites $RFeO_3$ (R=Lu, Er-Tb). Appl Phys Lett 2011;99:122502.

[285] Machlin ES, Chaudhari P. In: Machlin ES, Rowland TJ, editors. Synthesis and properties of metastable phases. Warrendale: The Metallurgical Society of AIME; 1980. p. 11–29.

[286] Flynn CP. Strain-assisted epitaxial growth of new ordered compounds. Phys Rev Lett 1986;57:599–602.

[287] Bruinsma R, Zangwill A. Structural transitions in epitaxial overlayers. J Phys (Paris) 1986;47:2055–73.

[288] Gorbenko OY, Samoilenkov SV, Graboy IE, Kaul AR. Epitaxial stabilization of oxides in thin films. Chem Mater 2002;14:4026–43.

[289] Rondinelli JM, Fennie CJ. Octahedral rotation-induced ferroelectricity in cation ordered perovskites. Adv Mater, in press.

[290] Fennie CJ. Ferroelectrically induced weak ferromagnetism by design. Phys Rev Lett 2008;100:167203.

[291] Varga T, Kumar A, Vlahos E, Denev S, Park M, Hong S, et al. Coexistence of weak ferromagnetism and ferroelectricity in the high pressure $LiNbO_3$-type phase of $FeTiO_3$. Phys Rev Lett 2009;103:047601.

[292] Singh-Bhalla G, Bell C, Ravichandran J, Siemons W, Hikita Y, Salahuddin S, et al. Built-in and induced polarization across LaAlO3/SrTiO3 heterojunctions. Nature Phys 2011;7:80–6.

[293] Dho J, Blamire MG. Competing functionality in multiferroic $YMnO_3$. Appl Phys Lett 2005;87:252504.

[294] Martí X, Sánchez F, Fontcuberta J, García-Cuenca MV, Ferrater C, Varela M. Exchange bias between magnetoelectric $YMnO_3$ and ferromagnetic $SrRuO_3$ epitaxial films. J Appl Phys 2006;99:08P302.

[295] Dho J, Qi X, Kim H, MacManus-Driscoll JL, Blamire MG. Large electric polarization and exchange bias in multiferroic $BiFeO_3$. Adv Mater 2006;18: 1445–8.

[296] Béa H, Bibes M, Cherifi S, Nolting F, Warot-Fonrose B, Fusil S, et al. Tunnel magnetoresistance and robust room temperature exchange bias with multiferroic $BiFeO_3$ epitaxial thin films. Appl Phys Lett 2006;89:242114.

[297] Martin LW, Chu YH, Zhan Q, Ramesh R, Han SJ, Wang SX, et al. Room temperature exchange bias and spin valves based on $BiFeO_3/SrRuO_3/SrTiO_3/Si$ (001) heterostructures. Appl Phys Lett 2007;91:172513.

[298] Borisov P, Hochstrat A, Chen X, Kleeman W, Binek C. Magnetoelectric switching of exchange bias. Phys Rev Lett 2005;94:117203.

[299] Laukhin V, Skumryev V, Martí X, Hrabovsky D, Sánchez F, García-Cuenca MV, et al. Electric-field control of exchange bias in multiferroic epitaxial heterostructures. Phys Rev Lett 2006;97:227201.

[300] Béa H, Bibes M, Ott F, Dupé B, Zhu XH, Petit S, et al. Mechanisms of exchange bias with multiferroic $BiFeO_3$ epitaxial thin films. Phys Rev Lett 2008;100: 017204.

[301] Chu YH, Martin LW, Holcomb MB, Gajek M, Han SJ, Balke N, et al. Electric-field control of local ferromagnetism using a magnetoelectric multiferroic. Nature Mater 2008;7:478–82.

[302] He X, Wang Y, Wu N, Caruso AN, Vescovo E, Belashchenko KD, et al. Robust isothermal electric control of exchange bias at room temperature. Nature Mater 2010;9:579–85.

[303] Yu P, Lee JS, Okamoto S, Rossell MD, Huijben M, Yang CH, et al. Interface ferromagnetism and orbital reconstruction in $BiFeO_3$-$La_{0.7}Sr_{0.3}MnO_3$ heterostructures. Phys Rev Lett 2010;105:027201.